

Conserved fatty acid profiles and lipid metabolic pathways in a tropical reef fish exposed to ocean warming – an adaptation mechanism of tolerant species?

Carolina Madeira^{1,2*}, Diana Madeira^{1,3}, Nemiah Ladd^{4,5}, Carsten J. Schubert⁴, Mário S. Diniz¹, Catarina Vinagre^{2,6}, Miguel C. Leal^{3,4}

¹UCIBIO – Applied Molecular Biosciences Unit, NOVA School of Science and Technology, 2829-516 Caparica, Portugal

²MARE – Marine and Environmental Sciences Centre, University of Lisbon, Campo Grande, 1749-016 Lisboa, Portugal

³CESAM – Centre for Environmental and Marine Studies, University of Aveiro, Edifício ECOMARE, Estrada do Porto de Pesca Costeira, 3830-565 Gafanha da Nazaré, Portugal

⁴Centre for Ecology, Evolution and Biogeochemistry, Swiss Federal Institute of Aquatic Science and Technology (Eawag), Seestrasse 79, 6047 Kastanienbaum, Switzerland

⁵Ecosystem Physiology, University of Freiburg, 53/54 Georges-Köhler Allee, 79119 Freiburg, Germany

⁶CCMAR - Centre of Marine Sciences, University of Algarve, Campus de Gambelas, 8005-139 Faro, Portugal

*Author for correspondence:

Carolina Madeira

e-mail: scg.madeira@fct.unl.pt; orcid: 0000-0003-1632-634X

Running title: Clownfish maintain stable fatty acid signatures at high temperature

Acknowledgements

Authors thank V. Mendonça for help during transport and accommodation of the fish. This work was funded by: i) the Portuguese Fundação para a Ciência e Tecnologia (FCT) through the projects PTDC/MAR-EST/2141/2012, UIDB/04292/2020 granted to MARE, UIDB/04326/2020 granted to CCMAR and UIDB/04378/2020 granted to UCIBIO; ii) CESAM (UIDP/50017/2020+UIDB/50017/2020) by FCT/MEC through national funds, and the co-funding by FEDER, within PT2020 Partnership Agreement and Compete 2020; iii) work in the organic chemistry laboratory at Eawag Kastanienbaum was funded by internal Eawag funds. CM was supported by a researcher grant CEECIND/01526/2018 provided by FCT. D.M. was supported by a researcher grant CEECIND/01250/2018, by FCT. M.L. was supported by the Integrated Programme of SR&TD “SmartBioR - Smart Valorization of Endogenous Marine Biological Resources Under a Changing Climate” (Centro-01-0145-FEDER-000018), co-funded by Centro 2020 program, Portugal 2020, European Union, through the European Regional Development Fund.

Author credit statement.

CV and MSD designed the study; MCL, NL and CJS planned and supervised fatty acid analysis; CV, MSD and MCL acquired funds; CM and DM performed animal experiments; CM performed lab analyses and wrote the first paper draft; CM, DM and MCL performed statistical analyses. All authors critically revised the manuscript, agreed with the author order and gave their final approval for publication. All authors agree to be accountable and take responsibility for accuracy and integrity of the research conducted.

Declaration of interest statement.

The authors declare that they have no conflict of interests.

Ethical statement.

All research conducted meets the ethical guidelines of the study country (Portugal) as well as of the European Union. Animal husbandry followed European Directive 2010/63/EU and

Portuguese Decree-Law 113/2013 from August 7th with regards to 'Protection of Animals for Scientific Purposes'. No wild endangered or otherwise subject of special protection specimens were used in the present study. CM, DM, CV and MSD are trained and licensed to conduct animal research.

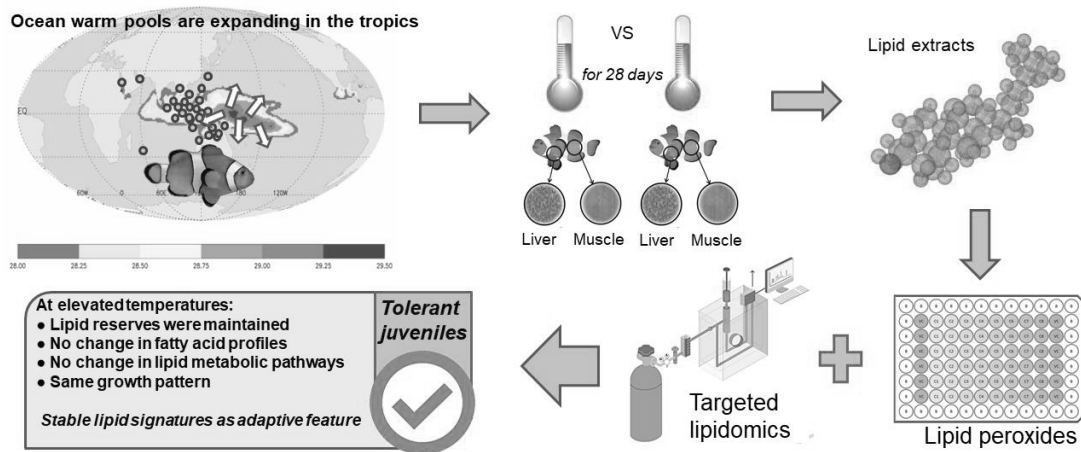
Data archiving statement.

To comply with scientific transparency policies and FAIR guidelines for data sharing and stewardship, raw data matrices from this study were stored in Zenodo (doi: 10.5281/zenodo.4582675) under an open access creative commons attribution 4.0 international license.

88 ABSTRACT

89 Climate warming is causing rapid spatial expansion of ocean warm pools from equatorial
90 latitudes towards the subtropics. Sedentary coral reef inhabitants in affected areas will thus
91 be trapped in high temperature regimes, which may become the “new normal”. In this
92 study, we used clownfish *Amphiprion ocellaris* as model organism to study reef fish
93 mechanisms of thermal adaptation and determine how high temperature affects multiple
94 lipid aspects that influence physiology and thermal tolerance. We exposed juvenile fish to
95 two different experimental conditions, implemented over 28 days: average tropical water
96 temperatures (26 °C, control) or average warm pool temperatures (30 °C). We then
97 performed several analyses on fish muscle and liver tissues: i) total lipid content (%), ii)
98 lipid peroxides, iii) fatty acid profiles, iv) lipid metabolic pathways, and v) weight as body
99 condition metric. Results showed that lipid storage capacity in *A. ocellaris* was not affected
100 by elevated temperature, even in the presence of lipid peroxides in both tissues assessed.
101 Additionally, fatty acid profiles were unresponsive to elevated temperature, and lipid
102 metabolic networks were consequently well conserved. Consistent with these results, we
103 did not observe changes in fish weight at elevated temperature. There were, however,
104 differences in fatty acid profiles between tissue types and over time. Liver showed
105 enhanced α -linolenic and linoleic acid metabolism, which is an important pathway in stress
106 response signaling and modulation on environmental changes. Temporal oscillations in
107 fatty acid profiles are most likely related to intrinsic factors such as growth, which leads to
108 the mobilization of energetic reserves between different tissues throughout time according
109 to organism needs. Based on these results, we propose that the stability of fatty acid
110 profiles and lipid metabolic pathways may be an important thermal adaptation feature of
111 fish exposed to warming environments.

112
113 Keywords: clownfish; warming environments; coral reefs; fatty acid profiling; lipid metabolic
114 networks



Highlights

- Effects of warm temperature on lipid profiles and pathways were tested in clownfish
- Muscle and liver were unresponsive to temperature change
- Lipid storage capacity was maintained, even with lipid peroxidation
- No change was detected in metabolic pathways at warm temperature
- Growth remained unchanged, suggesting ability to acclimate

1. Introduction

Oceans are a major heat sink for Earth's climate system (Herbert et al., 2010). Global warming has caused tropical oceans to warm by 0.8 °C to 1.6 °C in the past decades (IPCC, 2019). As a consequence, large fluctuations of ocean isotherms are also occurring, causing a rapid expansion of ocean warm pools (Arora et al., 2016). Areas with sea surface temperatures (SST) between 29 °C – 30 °C in tropical oceans and seas have increased at a rate of 2.29×10^6 km² per decade since the 1980s, whereas areas with SST between 26 °C and 28 °C have been contracting, and subtropical areas with SST below 25 °C have changed little (Lin et al., 2011). The distribution of tropical ocean temperatures is thus being skewed towards the warmer edge. Additional thermal pressures are expected to be exerted on marine ecosystems, with predicted future anomalies for the tropical regions in the range of + 0.9 °C to + 3.3 °C across the different climate warming scenarios for the late 21st century (2081-2100; IPCC, 2014, 2013).

Previous studies of marine organisms' responses to a warming environment have highlighted the importance of reorganizing biodiversity in space and time (Groom et al., 2012), with shifts in ecosystem structure and function (Bijma et al., 2013; Graham et al., 2008). For instance, tropical reef fish have been found to be "on the move", especially at the latitudinal limits of their distribution (S. Bejarano, pers. com.). This ongoing process depends on fish environmental tolerance limits as well as their capacity for adaptation and rates of molecular and phenotypic trait evolution (Bruneel et al., 2018; Payne et al., 2016; Rummer et al., 2014). However, ongoing expansion of ocean warm pools beyond areas of regular occurrence means that many tropical and subtropical fish populations and species, especially slow swimmers, or sedentary ones, may find themselves trapped and living permanently at or beyond the limits of their optimum tolerance range. Despite the high thermal tolerance of these ectotherms, it is not clear if such an environment will lead to increased thermal specialization and novel adaptations or to deleterious effects for already warm-adapted species. This knowledge is especially relevant given that species with low

capacity for movement and/or limited ability for further acclimation to heat may be disproportionately affected (Madeira et al., 2018; Roessig and Woodley, 2004).

The deleterious effects of high temperatures are usually a consequence of energetic tradeoffs at the organism level, theorized by Sokolova (2013) as energy-limited tolerance to stress. During stress, a higher energetic investment in physiological compensatory mechanisms occurs, at the expense of growth and reproductive output (Angilletta et al., 2003; Munday et al., 2012). This is explained by the loss of bioenergetics balance, in which an exhaustion of cellular energetic fuels occurs, with consequent changes in availability, structure and composition of the main energy reserves, namely lipids (Balogh et al., 2013; Valles-Regino et al., 2015; Wen et al., 2017). These effects are expected to cascade through the food web, with severe impacts for marine populations (Anacleto et al., 2014; Colombo et al., 2020). In fact, lipids provide the densest form of energy in marine ecosystems, but they are also very susceptible to oxidative damage arising from stressful conditions (Parrish, 2013). Higher trophic levels are expected to be the most impacted by a decrease in lipid quality and/or availability, because organisms will be left with no option but to feed on less nutritious food. For instance, Hixson and Arts (2016) suggested that ocean warming could lead to a worldwide reduction of omega-3 long-chain polyunsaturated fatty acids (FA) availability in marine organisms. These essential FA are mostly obtained through diet and have vital roles in cellular processes such as membrane remodeling and homeoviscous adaptation, determinants of thermo-sensitivity (Csoboz et al., 2013; and see also Ernst et al., 2016; Eghtesadi-Araghi and Bastami, 2011 and Sinensky, 1974 for a review). Additionally, essential FA play important roles in nutrient transport and enzyme activity (Neidleman, 1987). The decreased bioavailability of omega-3 FA under current warming conditions is already affecting the fitness of top predators (e.g. decreasing spawning and egg quality, fertilization and hatching rates, Rainuzzo et al., 1997) and consequently ecosystem stability (Colombo et al., 2020; Parrish, 2013).

In this context, the utility of systems-biology approaches, such as the large-scale study of lipids and their interactions, pathways and networks, coupled to computational methods, is useful for identifying metabolic state and organism health (Checa et al., 2015; Török et al., 2014). Specifically, targeted investigations of alterations in the composition and content of lipid classes like fatty acids provide information on physiological and pathological condition and facilitate mechanistic insights into changes in cellular function, biochemical mechanisms of stress and impaired health processes under climate warming.

Past studies have shown that both freshwater and marine fish exposed to higher temperatures usually i) decrease their overall body lipid content, e.g. Atlantic salmon *Salmo salar* (Ruyter et al., 2006; Todd et al., 2008); ii) decrease diversity in FA composition, e.g. duskytail grouper *Epinephelus bleekeri* (Dey et al., 1993); iii) decrease levels of polyunsaturated and long-chain polyunsaturated fatty acids (PUFA and HUFA) over time, e.g. seabass *Dicentrarchus labrax*, (Barbosa et al., 2017) ; iv) decrease levels of omega-3 FA, e.g. tuna *Thunnus alalunga*, (Pethybridge et al., 2015), v) increase overall levels of saturated fatty acids (SFA), e.g. golden mahseer *Tor putitora*, (Akhtar et al., 2014) and vi) have higher levels of polar lipids and decreased levels of neutral lipids (especially triglycerides) (e.g., seabass *D. labrax*, Bouaziz et al., 2017). These studies ultimately suggest that environmental variation leads to altered physiological phenotypes, with significant internal stoichiometry, metabolic and bioenergetic consequences. However, crucial knowledge gaps persist, especially with regards to the comprehension of the mechanisms and layers of molecular networks that underlie these changes. Advances are therefore needed to provide insights into the cellular regulatory pathways that determine phenotypic outcomes of marine organisms under climate change.

In this study, we profiled fatty acids of the model tropical reef fish *Amphiprion ocellaris* to understand how fatty acid metabolism shapes thermal acclimation and adaptation potential of shallow water, sedentary tropical fish to a warmer environment. We have previously shown that *A. ocellaris* responds to temperature increase by upregulating the cellular stress

response in muscle, gills and liver (Madeira et al. 2016). As a follow-up, fatty acid profiles, pathways and networks, as well as lipid contents and lipid peroxides, anchored in body condition metrics (weight) were assessed in fish exposed to control (26 °C) and warmer conditions (30 °C) in order to test the following hypotheses: H1) different tissues show variable susceptibility to variation in lipid composition and metabolism under high temperature; H2) tissues show reduced lipid contents as consequence of temperature-induced lipid peroxidation damage and higher bioenergetic costs to maintain homeostasis; H3) FA profiles display changes in saturated and unsaturated fatty acids as temperature increases; H4) omega-3 FA concentrations decrease, whereas omega-6 FA concentrations increase at high temperature, with cascading consequences for metabolic pathways.

2. Materials and methods

2.1. Animal housing

We selected the Pomacentridae fish *Amphiprion ocellaris* as study species since it has proven to be a suitable model for climate change studies (Madeira et al., 2016; Madeira et al., 2017). It is also a well-established ornamental aquaculture species, easy to obtain, with simple handling and care (Khoo et al., 2018; Vargas et al., 2016). Ocellaris clownfish have a bi-phasic life cycle with an oceanic larval phase (2 weeks) and a reef benthic phase in juvenile (post-recruitment), adult and embryo stages, in which the fish live symbiotically with their host sea anemones (Roux et al., 2019). Clownfish live in groups, in a dominance-based social hierarchy composed of a breeding pair and several smaller non-breeding male fish. The adults have an average life-span of 6-10 years in the wild (Fautin and Allen, 1992). Three-month old juvenile fish (N = 48, weight 1.05 ± 0.28 g, length 3.54 ± 0.36 cm) were purchased at the Tropical Marine Centre Iberia hatchery (Loures, Portugal) and placed in a marine life-support system upon arrival at experimental facilities, where they were acclimated for two weeks at a constant temperature of 26 ± 0.5 °C.

2.2. Experimental setup

During experiment trials, 26 ± 0.5 °C was set as the control temperature, which represents the average water temperature at which *A. ocellaris* lives (Allen, 2009; Madeira et al., 2017). Additionally, this temperature also reflects the thermal history conditions of our specimens – clownfish from the hatchery were reared at this temperature, as well as the original brood stock. The high temperature treatment was set at 30 ± 0.5 °C, which corresponds to warm pool temperatures, at the limit of *A. ocellaris*' native thermal range (22 °C – 30 °C, Allen, 2009; Madeira et al., 2017). The aquaria system consisted of an indoor re-circulating volume of 2,000 L, with filtered and aerated seawater. It comprised six polyvinyl tanks (dimensions 35 x 35 x 55 cm), one common sump, an external skimmer and a UV filter. Tanks were the experimental units, with three replicates for each temperature condition ($N = 8$ animals.tank⁻¹, mirroring density of fish in nature in a single host anemone). Fish were fed twice a day with a mixture of frozen and dry food (shrimp, mussels and *Spirulina* pellets in proportion 1:1:1 weight). Salinity was kept at 35 ppt (measured once a day); pH at 8 ± 0.01 , ammonia below < 0.1 mg.l⁻¹ and nitrites below 0.3 mg.l⁻¹ (measured once a week). The light-dark cycle was kept at 12L:12D. Animal sampling was performed once *per* week for 28 days. Five specimens were randomly sampled on day 0 from both treatments as an overall baseline control (before any change in temperature), euthanized by cervical dissection, measured, weighed, and muscle and liver tissues dissected and frozen at -80 °C. Water temperature in the high temperature treatment tanks was then increased at a rate of 0.10 °C.hr⁻¹, maintained with thermostat heaters (ELITE 200W) and continuously monitored with Petco thermometers (UK). On days 7, 14, 21 and 28, three to five specimens from each temperature (control and high temperature) were sampled as previously described ($N_{\text{total}} = 3\text{-}5$ specimens \times 5 timepoints \times 2 treatments = 38 specimens sampled in total).

2.3. Total lipid extraction and quantification

All glassware used in this protocol was combusted prior to use at 450 °C for 5 h. Tissue samples ($N_{\text{total}} = 38$ specimens \times 2 tissues = 76 samples) were freeze-dried and ground to

a fine homogeneous powder. Lipids from 2-5 mg and 10-30 mg of tissue (liver and muscle, respectively) were extracted with 1 ml of 2:1 dichloromethane:methanol (DCM:MeOH), vortexed for 5 s and sonicated for 10 min in an ice-cold water bath. Samples were then frozen at -20 °C overnight to allow the settlement of tissue particles in the solvent. The supernatant from each sample was then transferred to new glass vials with glass pipettes and the resulting total lipid extracts (TL) were evaporated to dryness under a stream of N₂. All the previous extraction steps were repeated at least three times for each sample. Lipid content (LC) in each sample was then calculated as follows:

$$\%LC = (\text{Weight}_{\text{TL}} \div \text{Weight}_{\text{tissue sample}}) \times 100$$

2.4. Lipid peroxidation levels

Tissue samples ($N_{\text{total}} = 38 \text{ specimens} \times 2 \text{ tissues} = 76 \text{ samples}$) were homogenized in 1 ml of phosphate buffer saline (140 mM NaCl, 3 mM KCl, 10 mM Na₂HPO₄, 2 mM KH₂PO₄, pH 7.4) using a Tissue Master 125 homogenizer on ice. The crude homogenates were then centrifuged at 4 °C for 15 min at 10,000 × g. The supernatants were collected, transferred to new microtubes and frozen immediately (-80 °C). The lipid peroxides assay was adapted from the thiobarbituric acid reactive substances (TBARS) protocol (Uchiyama and Mihara, 1978). In brief, five µl of each sample were diluted in 45 µl of 50 mM NaH₂PO₄ buffer. Then, 12.5 µl of SDS 8.1 %, 93.5 µl of trichloroacetic acid 20 % and 93.5 µl of thiobarbituric acid 1 % were added, together with 50.5 µl of ultrapure water before vortexing the microtubes for 30 s, followed by an incubation in boiling water for 10 min. Samples were afterwards placed on ice for a few minutes to cool, 62.5 µl of Milli-Q grade ultrapure water were added and absorbance was read at 530 nm in a microplate reader (Benchmark, Bio-Rad). To quantify the lipid peroxides, an eight-point calibration curve (0 to 0.3 µM TBARS) was calculated using malondialdehyde bis (dimethylacetal) standards (Merck). Lipid peroxides results were then normalized per mg of TL.

2.5. Clownfish fatty acids profiling

For fatty acid profiling, 50 μ l of a recovery standard with *n*-C_{19:0} alkanolic acid in ethyl acetate were quantitatively added to the TL of each sample ($N_{\text{total}} = 38 \text{ specimens} \times 2 \text{ tissues} = 76 \text{ samples}$). TL were then methylated to produce fatty acid methyl esters (FAMES) using 1 ml of BF₃ in MeOH (14% by volume, Sigma Aldrich), sonicated for 5 min and placed in an oven for 2 h at 100 °C. After adding 2 ml of nanopure water, FAMES were extracted with 1 ml hexane, vortexed and then centrifuged for 3 min at 1500 rpm to accelerate the separation process. The hexane phase of each sample was collected into new vials. Extraction of FAMES with hexane rinses was repeated at least three times. Samples were then blown down to dryness with a N₂ stream and dissolved in 300 μ l of ethyl acetate prior to quantification of FAMES by gas chromatography with a flame ionization detector (GC-FID) (GC-2010 Plus, Shimadzu, Japan). An AOC-20i autosampler (Shimadzu) injected the samples through a split/splitless injector operated in splitless mode at 280°C. The GC column was an InertCap 5MS/NP column (30 m; 0.25 mm; 0.25 μ m; GL Sciences, Japan). The GC oven program heated from 70 °C to 130 °C at 20 °C.min⁻¹ and then from 130 °C to 320 °C at 4 °C.min⁻¹ and held for 20 min. The GC-FID limit of detection (LOD) was 20 ng. μ l⁻¹ for all FA. All compounds were quantified relative to the *n*-C_{19:0} fatty acid recovery standard and the final concentration expressed as μ g.mg⁻¹ of dry weight. Compounds were identified by comparing their retention times to those of laboratory standards (Supelco 37 Component FAME Mix, ref. CRM47885). Samples with unidentified compounds were further analyzed under identical chromatographic conditions by gas chromatography–mass spectrometry (GC–MS) with a QP2020 mass spectrometer (Shimadzu) and comparing the resulting mass spectra to reference spectra in the National Institute of Standards and Technology (NIST) library.

2.6. Data analysis

2.6.1. Fish body condition: weight

Body mass (g) was analyzed for outliers (box-whiskers plot) and tested for normality (Shapiro's Wilk test) and homoscedasticity (Levene's test). Following assumptions, the

effects of acclimating temperature on weight were tested with a Student's t-test ($p < 0.05$ for significance).

2.6.2. Lipid contents and lipid peroxides

For lipid contents and lipid peroxides, data were first tested for outliers (box-whiskers plot), normality (Shapiro's Wilk test) and homoscedasticity (Levene's test). To test if there was a relationship between the extent of lipid peroxidation and a change in capacity for lipid storage (as consequence of changes in metabolism with acclimating temperature), an ANCOVA with a separate slope design was used, as lipid peroxides levels and temperature are not independent. Analyses were done in STATISTICA v8 (Statsoft, USA).

2.6.3. Fatty acid profiles and data mining

Data matrices were pre-processed before statistical analysis. Datasets were assessed and treated for missing data (MD) in MetImp v1.2 (free available web tool, <https://metabolomics.cc.hawaii.edu/software/MetImp/>). A group-wise missing filter was initially applied, eliminating all FAs with over 50 % MD. Then, MD imputation, which is a standard procedure in GC data, as coherent and complete data matrices are a pre-requisite for accurate and reliable statistical analysis (Kokla et al., 2019), was performed. To input missing values to the remaining FA variables (16.45 % MD in the total dataset), we followed the protocol established by Wei et al., (2018) for GC-MS data, and the MCAR/MAR (Missing Completely at Random/Missing at Random) algorithm, based on random-forests (with seed 1234) was used for this purpose.

The final data matrix was composed of 26 FA (Table 1) plus 9 added variables, consisting of FA summed into different classes and 3 variables consisting of FA ratios, yielding 38 variables in total. The two latter included (i) SFA (0 double bonds: 14:0, 15:0, 16:0, 17:0, 18:0, 20:0 and 22:0), (ii) MUFA (monounsaturated fatty acids, 1 double bond: 16:1n-7, 17:1n-7, 18:1n-9 *cis* and *trans*, 19:1n-9, 20:1n-9, 24:1n-9), (iii) PUFA (2-3 double bonds: 18:2n-6 *cis* and *trans*, 20:3n-3, 20:3n-6, 22:2n-6, 26:2n-6, 27:2), (iv) HUFA (highly

unsaturated fatty acids, ≥ 4 double bonds: 20:5n-3, 20:4n-6, 22:6n-3, 22:5n-3, 22:4n-6), (v) omega-3 fatty acids (double bond three atoms away from the terminal methyl group: 20:3n-3, 20:5n-3, 22:6n-3, 22:5n-3), (vi) omega-6 fatty acids (double bond six atoms away from the terminal methyl group: 18:2n-6 *cis* and *trans*, 20:3n-6, 20:4n-6, 22:2n-6, 22:4n-6, 26:2n-6), (vii) omega-7 fatty acids (double bond seven atoms away from the terminal methyl group: 16:1n-7 and 17:1n-7); (viii) omega-9 fatty acids (double bond nine atoms away from the terminal methyl group: 18:1n-9 *cis* and *trans*, 19:1n-9, 20:1n-9, 24:1n-9), (ix) total sum of all FA, and lastly fatty acid ratios (x) ARA/EPA (arachidonic acid 20:4n-6/eicosapentanoic acid 20:5n-3), (xi) EPA/DHA (eicosapentanoic acid 20:5n-3/docosahexaenoic acid 22:6n-3) and (xii) $\sum n-6/\sum n-3$. The complete dataset was log-transformed and auto-scaled (mean centered and divided by the standard deviation of each variable) prior to statistical analyses.

With the aim of identifying the main and interactive effects of (i) temperature, (ii) tissue and (iii) time in FA profiles and classes, as well as the FA variables that contribute to the differences found, several multivariate analyses were performed. An unsupervised principal components analysis (PCA) was applied to explore FA data structure, followed by heat maps with hierarchical clustering of FA classes, constructed based on the following metrics (i) distance measure: Pearson correlation (similarity of expression profiles), (ii) clustering algorithm: complete linkage (forms compact clusters), (iii) feature auto-scale. These analyses were run in Metaboanalyst v4.0 (<https://www.metaboanalyst.ca/>) (Chong et al., 2019). A PERMANOVA analysis was then run using PERMANOVA+ v1.0.6 as implemented in PRIMER v6.1.16. A resemblance matrix was calculated based on Euclidean distances, and the analysis was based on Type III SS for unbalanced designs, with 9999 permutations of residuals under a reduced model. For factors and interaction of factors (with more than two factor categories) significantly affecting FA profiles, pairwise tests were employed to test which groups were different. A SIMPER analysis was also run to identify contributions from each FA and FA classes to the significant differences found for main factors in the PERMANOVA.

398

399 2.6.4. Fatty acid quantitative enrichment and pathway analysis

400 Functional enrichment and pathway analysis were performed only for relevant factors that
401 displayed significant effects on overall FA profiles of *A. ocellaris*, as detected by
402 PERMANOVA analysis. The objective was to gain biological insights into the functional
403 roles of pre-defined subsets of FA analytes in animal metabolism and physiology (Ma et al.,
404 2019). To define the set of individual FA variables to be enriched, a threshold was defined
405 based on the following criterion: within a significant factor effect, fatty acids identified in the
406 SIMPER analysis as contributing up to a cumulative percentage of 90% for the observed
407 differences were selected for analysis. Lipid annotation was then performed, based on
408 LIPID MAPS for chemical structure and KEGG (Kyoto Encyclopedia of Genes and
409 Genomes) as well as HMDB (Human Metabolome Database) for function (Fahy et al.,
410 2007; Kanehisa et al., 2017; Züllig et al., 2020). Only well annotated FA were mapped.
411 Functional enrichment and pathway analysis were then performed in Metaboanalyst v4.0
412 (Chong et al., 2019).

413

414 Quantitative enrichment analysis (QEA) was performed by setting the '*normal metabolic*
415 *pathways*' based on SMPDB (Small Molecule Pathway Database) metabolite library
416 (Frolkis et al., 2009; Jewison et al., 2014). The analysis was done based on FA
417 concentration and annotation, using the global test algorithm, in which a generalized linear
418 model is used to estimate a Q-statistic for the FA set (with FDR corrected p-values), to
419 describe the correlation between compound concentration profiles and phenotypes, as well
420 as list the different metabolic pathways in which each FA takes part. Pathway topology
421 analysis was also performed by selecting the pathway libraries from SMPDB (Howe et al.,
422 2013) and was based on two features (i) quantitative functional enrichment (described
423 previously, significant if $FDR < 0.05$) and (ii) pathway topology analysis to estimate node
424 importance. This analysis was implemented using the relative betweenness centrality, which
425 takes into account the role of the FA, position and direction of the interaction, measuring
426 the centrality of a given FA in the metabolic network (and ultimately gives information about

the relative importance or role of the FA in the organization of the metabolic network, see Xia and Wishart, 2010 for further details). The pathway impact was considered relevant if > 0.1.

3. Results

3.1. Body condition

Animals' weight (mean \pm SD) was similar between temperature treatments after 28 days of the experiment. Individuals raised at 26 °C had an average body mass of 1.09 ± 0.26 g, whereas individuals raised at 30 °C had an average body mass of 1.06 ± 0.30 g (t-test = 0.404, p-value = 0.688).

3.2. Total lipids and lipid peroxidation levels

Results of the ANCOVA model with separate slopes suggest that there are no significant changes in lipid contents in response to temperature in covariation with lipid peroxide (LPO) levels, both in muscle (test of whole model multiple R = 0.270, F = 0.870, p-value = 0.466) and liver (test of whole model multiple R = 0.398, F = 1.949, p-value = 0.142). Results indicate that both intercepts (temperature, F = 2.424, p-value = 0.129 for muscle, and F = 0.811, p-value = 0.375 for liver) and slopes (temperature \times LPO, F = 1.035, p-value = 0.336 for muscle and F = 2.694, p-value = 0.083 for liver) are statistically equal, showing that there is the same amount of lipid contents when there are no lipid peroxides at both temperatures and that the rate of lipid content change per unit of lipid peroxides is also the same at 26 °C and at 30 °C.

3.3. Fatty acid profiles

The list of FA analyzed in this study is presented in Table 1 (for complete data matrices with mean \pm SD fatty acid masses at different temperatures, tissues and times see supplemental material, Tables S1 and S2). The most abundant FA in *A. ocellaris* liver

tissue were palmitic acid, stearic acid, linoleic acid and oleic acid (16:0, 18:0, 18:2n-6c and 18:1n-9c, respectively), whereas palmitic acid, linoleic acid, oleic acid and docosahexaenoic acid (16:0, 18:2n-6t, 18:1n-9c and 22:6n-3 respectively) were the most abundant in muscle tissue (see Tables S1 and S2). Results from PCA analyses, in which FA were plotted grouped by factors (cumulative explained variance of 69.5 % for PC1 and PC2) showed i) no specific patterns for temperature groups (Fig. 1), ii) two clear clusters separating muscle from liver (Fig. 2), and also iii) no specific patterns for time groups (Fig. 3). Additionally, FA 14:0, 16:1n-7, 18:2n-6, 18:1n-9, 20:5n-3, 20:3n-6, 20:2n-3 and 20:1n-9 were all positively correlated, which in turn were negatively correlated to 18:0, 17:0, 22:5n-3, 22:0, 24:1n-9, 26:2n-6 and 27:2. The collective behavior of these FA is mainly represented by PC1. PC2 is influenced most by FA 15:0, 19:1n9, and 24:0, which are positively correlated, and 20:4n-6, 22:5n6, 22:4n6, 22:2n-6, which were negatively correlated to the previous ones (see Fig. S3 of PCA biplot in supplemental material).

In the heat map analyses of FA classes in response to temperature, results showed an increasing trend of omega-3, -6, -7 and -9, as well as SFA, PUFA and HUFA at elevated temperature, but a decreasing trend of MUFA and EPA/DHA as well as ARA/EPA ratios (Fig. 1). Trends in FA classes between different tissues (Fig. 2) showed that liver displayed higher concentrations of all classes and ratios when compared to muscle, except for ARA/EPA ratio, which was higher in muscle. Finally, trends in FA classes between time groups (Fig. 3) suggest oscillations in FA concentration along time, with higher concentrations at T0, T14 and T28, and lower overall concentrations at T7 and T21.

Multi-factorial PERMANOVA testing the effects of temperature, tissue and time on fatty acids and fatty acid classes and ratios showed significant differences for tissue (Pseudo-F = 61.091, $P(\text{perm}) < 0.001$), time (Pseudo-F = 2.394, $P(\text{perm}) = 0.004$) and the interaction of both (Pseudo-F = 1.966, $P(\text{perm}) = 0.017$) (Table 2). No significant differences were found for temperature effects, or interactions of time and tissue with temperature. Pairwise tests for time groups indicated that T14 was different from the rest of time levels except for

T0 (T7 vs. T14, $P(\text{perm}) = 0.004$; T14 vs. T21, $P(\text{perm}) = 0.001$; T14 vs. T28, $P(\text{perm}) = 0.028$). No other differences were found between pairwise combinations of T0, T7, T21 and T28. Moreover, pairwise tests for the interaction of tissue with time showed that liver was different from muscle at all time levels (T0, T7, T14, T21 and T28 all had $P(\text{perm}) < 0.001$) and that within liver, T0 differed from T7 ($P(\text{perm}) = 0.045$) and that T14 was also different from the remaining time levels (T0 vs. T14, $P(\text{perm}) = 0.005$; T7 vs. T14, $P(\text{perm}) = 0.001$; T14 vs. T21, $P(\text{perm}) = 0.007$; T14 vs. T28, $P(\text{perm}) = 0.002$). Within muscle, no differences were detected along time, from T0 to T28.

Results from SIMPER analysis are presented in Table 3 for the effects of independent factors tissue and time on FA profiles. Up to 90 % of cumulative FA contribution to significant differences observed among tissues and among time levels was homogenously distributed between 25 and 31 fatty acid variables, out of the 38 analyzed. The top five variables contributing to tissue differences were 27:2, 18:0, 26:2n-6, 17:0 and ΣSFA , whereas the top five variables contributing to multiple significant time comparisons were: 14:0, 20:3n-3+20:3n-6, 16:1n-7, 19:1n-9 and 20:5n-3 (Table 3).

3.4. Quantitative functional enrichment and pathway analysis

Based on PERMANOVA results, enrichment and pathway analysis were performed for significant effects of tissue on FA profiles. Since no significant effects of temperature were detected in FA concentrations, this implies that there are also no significant changes in FA pathway topology or function under elevated temperature, when compared to the control temperature. Effects of time, although significant on FA profiles, were not used in these analyses, as oscillation of FA concentration along time is a regular occurrence of minor interest to the objectives of this research.

Functional enrichment and pathway analysis were based on 20 FA for differences between tissues. QEA identified 9 relevant metabolic pathways that showed significant differences between liver and muscle tissues ($\text{FDR} < 1.0\text{E-}12$, Fig. 4). Among these pathways, the

most relevant was α -linolenic and linoleic acid metabolism with an impact of 0.25 for topology, indicating that the involved FA (C18:2n-6c, C20:5n-3, C20:3n-6, C22:6n-3, C22:5n-3, see Table S3) are central metabolites in this pathway.

4. Discussion

As modulators of biological membrane properties, lipids play a vital role in physiological stress management and capacity for adaptive responses in the face of climate change (Eghtesadi-Araghi and Bastami, 2011; Ernst et al., 2016). Here, we tested whether a tropical shallow-water reef fish, *A. ocellaris*, displays thermal adaptations at the lipid level that enable it to sustain elevated environmental temperatures. Specifically, we investigated temperature induced changes in total lipids, lipid peroxidation, fatty acid profiles and metabolic pathways in fish tissues that may signal either acclimation and tolerance or impaired health processes (see Balogh et al., 2013; Neidleman, 1987), coupled to weight assessments. Our main purpose was to evaluate warm-adapted species heat coping strategies under ocean warm pool expansion scenarios.

Stability of lipid signatures as a thermal adaptation mechanism of juvenile clownfish

Overall, our results showed that bioenergetic balance, as well as fatty acid concentrations, chain lengths and lipid metabolic pathways remained mostly unchanged under elevated temperature in the studied tropical reef fish. Additionally, even with increasing levels of lipid peroxides under elevated temperature, overall lipid contents in *A. ocellaris* were unchanged and lipid accumulation rates also remained the same at 26 °C and 30 °C. This suggests that lipid peroxide levels measured in muscle and liver tissues at elevated temperature were merely a reflection of faster metabolism and higher respiration rates that occur during acclimation to high temperature, given that no energy tradeoff was observed. In fact, several authors have suggested that lipid peroxides, which occur mostly on phospholipids, PUFA, glycolipids and cholesterol (Ayala et al., 2014; Parrish, 2013), may act as crucial signaling molecules that initiate stress protein responses and membrane remodeling to

control the extent of cellular thermo-sensitivity (Csoboz et al., 2013; Liu et al., 2020), which was described by Török et al. (2014) as the 'membrane sensor hypothesis'. When stress levels remain below the threshold level of deleterious effects or when animals display increased resistance to peroxidation (Munro and Blier, 2012), an acclimation process is therefore induced until a new stage of physiological homeostasis is attained. This process is temporary and usually lasts between 1 to 3 weeks (Lesser, 2006; Okazaki and Saito, 2014), a duration similar to our experiment trials. According to previous studies with clownfish (see Madeira et al. 2016, 2017), a time-dependent induction of the heat stress response did occur in the presence of lipid peroxides at 30 °C (e.g. induction of Hsp70 and antioxidant enzymes such as catalase), which eventually resulted in full acclimation of this species. Interestingly, previous studies have also suggested that peroxidation index and longevity are negatively correlated in many vertebrate animals (Christen et al., 2020; Munro and Blier, 2012), and ocellaris clownfish are known to live up to 10 years in the wild. This is a considerable lifespan in comparison with other coral reef fish species and may be partially related to generally low peroxidation levels for this species.

Moreover, FA profiles remained similar between temperature treatments and no interactions of temperature with tissue type were detected. We also observed that concentrations of unsaturated fatty acids as well as of saturated fatty acids between temperature treatments remained stable, contrary to what would be expected during adjustments of lipid properties under temperature change. These adjustments in fatty acid saturation levels are crucial for plastic changes in cell membrane rigidity, thickness and relative hydrophobicity (Neidleman, 1987). Nevertheless, it is worth noting that Hernando et al. (2018) found that the maintenance of a stable unsaturated to saturated FA ratio actually seemed to be important to mitigate lipid damage under environmental stress, but there is still no clear consensus on the underlying biological pathways.

The assessed tissue of ocellaris clownfish contained low overall levels of HUFA (~ 13 % of total FA), which are the most susceptible to warming as they lead to higher production of

reactive alkyls that induce denaturation of functionally important biomolecules (Christen et al., 2020; Valles-regino et al., 2015). This characteristic coupled to i) low overall EPA levels (< 1 % of total FA in both tissues) which have been found to increase thermal resistance (Christen et al., 2020) (for instance in contrast to Atlantic salmon which has ~ 5 % EPA in total muscle FA and is considered rich in n-3 EPA contents, Horn et al., 2020), and to ii) high overall MUFA levels (~ 17 % of total FA), which are preferential fuels for energy metabolism in fish (Sidell et al., 1995) and play a significant role in maintaining ATP levels can explain juvenile clownfish tolerance to elevated temperature. Indeed, we found no further evidence of alteration in lipid metabolic pathways in clownfish at 30 °C in the assessed life-stage.

The maintenance of FA ratios among temperature treatments corroborates our previous results, given that altered ratios of different omega fatty acids can signal physiological imbalance. For instance, maintaining high levels of n-7 fatty acids is thought to improve heart function in vertebrates (Vannice and Rasmussen, 2014). This is an important feature for ectothermic animals, given that heart function relies on tissue aerobic capacity (Christen et al., 2020), and high temperatures lead to increased heart rate and oxygen demand (Pörtner et al., 2004). Moreover, n-9, n-6 and n-3 fatty acids are important mediators in pro- and anti-inflammatory pathways, which are usually triggered by higher availability and/or oxidation of fatty acids (Calder, 2011, 2010). Therefore, these FA play significant roles in stress responses. For instance, a balanced EPA/DHA ratio is thought to be efficient at reducing changes in ROS and for curtailing systemic inflammation, as the metabolization of n-3 FA gives rise to resolvins, which have powerful anti-inflammatory action (Calder, 2012, 2011). On the other hand, an increase in ARA/EPA ratio leads to a cascade of pro-inflammatory effects (e.g. ARA is a precursor of inflammatory prostaglandins and leukotrienes as well as proapoptotic metabolites) (Christen et al., 2020; Innes and Calder, 2018). Therefore, the stability of such FA ratios suggests that a healthy and balanced metabolism was maintained in fish at 30 °C. Similarly, Coleman et al., (2019) found that health, tissue biochemistry and nutritional properties of the yellowfin bream (*Acanthopagrus*

australis) were unaffected under near-future temperature conditions. The authors suggest that this may be an evolutionary consequence of species inhabiting environmentally challenging conditions, as may be the case for species inhabiting shallow coral reefs.

Additionally, this fish species showed no signs of weight changes after 28 days of exposure to 30 °C. The combination of these results suggests that juvenile *A. ocellaris* has the ability to persist in an elevated temperature regime. The thermal tolerance of this species' life-stage had also been observed in a previous study that evaluated juvenile *A. ocellaris* thermal preference, thermal limits and aerobic scope. Indeed, Velasco-Blanco et al., (2019), showed a thermal window width of 301.5 °C² and a critical thermal maximum of 34 °C to 40 °C for juvenile clownfish (depending on acclimation temperature). This clearly evidences eurythermal characteristics for this life-stage. As Christen et al., (2020) noted, it may well be that upper thermal limits are potentially related to cell and organelle membranes robustness against oxidation and maintenance of lipid peroxide levels below deleterious thresholds, as observed in this study. Nevertheless, other authors have observed that juveniles' growth rate and condition at high temperature in related *Amphiprion* spp. seem to vary widely (Rushworth et al., 2011).

It should be noted that this life stage is known to be more tolerant to heat than larvae or adults (e.g., as shown for *Sparus aurata*, Madeira et al., 2020), as juveniles generally have wider thermal windows (Dahlke et al., 2020). This is relevant considering that *A. ocellaris* is likely more exposed to high temperatures during the reef phase of its life cycle (that includes juveniles, adults and embryos) where it inhabits shallow waters, when compared to the oceanic larval phase. Within the reef phase, we expect that embryos and spawning adults may possibly display higher vulnerabilities than juveniles, as the latter seem to be well-equipped to deal with changing environmental conditions, as would be expected from a life-stage that is ready to settle in new reef environments. Interestingly, other studies with species from the *Amphiprion* genus have shown that adults exposed to 30 °C had reduced reproductive output (*A. melanopus*, Miller et al., 2015) and that adult dominant behavior

and aggression towards conspecifics seems to be accentuated with increasing temperature (A. *latezonatus*, Rushworth et al., 2011), which may result in higher mortality. To corroborate this, a recent meta-analysis by Dahlke et al., (2020) of 694 marine and freshwater fish species from all climatic zones showed that the adult mature stage is often the most sensitive to environmental challenges in the life cycle of a fish, as temperature requirements for reproduction and energetic trade-offs represent a critical bottleneck at this stage. Additionally, recent research has shown that (i) temperature effects on reproduction are modulated by nutritional status in coral reef fish (Donelson et al. 2010), and (ii) long-term thermal stress may cause decreased egg and sperm quality and viability in reef fish, including *Amphiprion* species (Miller et al., 2015). This is partially associated with reduced lipid reserves and yolk volume and/or lack of adequate fish nutrition (Bobe, 2015). There may even be a complete inhibition of reproduction in species that are constrained in their capacity to shift geographic range (Pankhurst and Munday, 2011), as is the case of coral-reef dependent species. Ultimately, thermal stress in the most severe cases can lead to a disarrangement of compensatory restructuring of FA in fish tissues, causing health impairments, organ failure and death (Liu et al., 2020). Given that our experiments only lasted for 28 days, it is unknown whether longer exposures could have different outcomes. We emphasize that other life-stages would have to be evaluated before conclusions can be drawn on the overall species tolerance level, warranting further studies in *A. ocellaris*.

Finally, the increase in temperature tested in this study is still within the thermal range of the species as a whole (22 °C – 30 °C) and can be experienced by fish populations in specific locations. Thus, a 4 °C increase in temperature may be an abiotic change that clownfish can broadly tolerate, except possibly at its lowest latitude limit. If 30 °C were to become the “new normal” for this fish species, it would be relevant to investigate whether population thermal history and local adaptation comparing the center to the edge of the distribution range populations leads to distinct response patterns and thermal adaptation ability. Moreover, if temperature further increases up to 32 °C during El Niño events, organisms may switch from a physiological compensation strategy (i.e., allocation of energy

to cellular defenses, repair mechanisms and molecular adjustments) to a metabolic conservation strategy (i.e., blocking stress responses, with severe deleterious effects) (see Petitjean et al., 2019). In the second option, severe thermal stress would likely lead to a depletion of lipid reserves with a loss of lipid storage capacity due to bioenergetic imbalance and lipid damage (Klepsatel et al., 2016), causing sublethal stress and animal mortality.

Enhanced lipid metabolic pathways: muscle vs. liver

The overall amount of lipid contents was higher in liver in comparison to muscle, as were the overall concentrations of each FA per mg of dry tissue, demonstrating that this organ is an important source of these biomolecules, similarly to other marine and freshwater fish (e.g. *Pagellus acarne*, *Sardina pilchardus*, *Trachinus draco*, Guil-Guerrero et al., 2011 and *Salmo trutta macrostigma*, Haliloğlu et al., 2011). However, this natural richness in lipids did not seem to increase the thermo-sensitivity of liver tissue, contrary to what most literature suggests (e.g. see study by Sun et al., 2019 with freshwater fish *Cyprinus carpio*).

The differences found in fatty acid profiles between muscle and liver tissues were mainly related to the abundance of long chain fatty acids, which had higher concentrations in liver. Most FA in animal tissues is usually composed of 16 to 18 carbons (Sargent et al., 1997), which are dietary FA, and the way in which these and the other FA produced by the organism are then used by the various organs is reflected in their structure and function. In liver, which is the main organ where FA are synthesized, stored and metabolized (Boglino et al., 2012; Guil-Guerrero et al., 2011; Haliloğlu et al., 2011), we found higher relative proportions of SFA and PUFA, although absolute concentrations of all FA classes were higher per mg of liver tissue. In contrast, muscle had higher relative proportions of MUFA, PUFA and HUFA, when compared to other FA classes. This may be related to the fact that muscle metabolism presents a considerable degree of flexibility. Although glycolysis is the main pathway for energy production in this tissue, thermogenic functions in muscle may lead to lipid uptake, with FA mobilization from storage to active sites under mild exercise, or

during starvation when glycogen reserves are not readily available, or even during overfeeding, as lipid oversupply inhibits glucose oxidation (Hocquette et al., 2010; Morales et al., 2017; Sheridan, 1988). These differences in organ function and metabolic pathways explain the differences we found between their FA profiles.

Our results from pathway analysis with gene enrichment tools between tissues confirm variability in metabolic pathways, as the differences found were mainly related to fatty acid biosynthesis (which occurs mostly in liver) and β -oxidation (which occurs in muscle). Nevertheless, the most impactful pathway was α -linolenic and linoleic acid metabolism, which was enhanced in liver. This pathway leads to the formation of omega-3 and omega-6 fatty acids through a series of conversions of the precursors α -linolenic and linoleic acid (respectively), which are then metabolized into a series of short-lived metabolites (eicosanoids) that act as signaling molecules in cells (Salway, 2013). These eicosanoids play important roles in stress responses (autocrine, paracrine and endocrine functions, e.g. mounting or inhibiting inflammation and other immune responses, changes in ion transport, regulation of cell growth and blood flow to tissues, see Calder, 2011; Calder, 1998). The enhancement of this pathway in liver when compared to muscle of *A. ocellaris* therefore suggests that liver tissue may be significantly involved in acclimation and maintenance of homeostasis during environmental stress.

Temporal oscillations in FA profiles

Our results showed significant temporal variations in FA profile throughout the experiment (with 28 FA contributing to 90 % of differences found), and interactions between time and tissue indicated that these occurred mainly in liver during the first two weeks of the experiment. Arguably, liver serves a major role in lipid storage especially in slow swimming teleost fish (Braekkan, 1959), as is the case of ocellaris clownfish. More importantly, liver is the interface between exogenous and endogenous fatty acid interorgan transport loops in fish (Sheridan, 1988). For instance, liver repackages dietary lipids and combines it with *de novo* synthesized lipids and carrier proteins for transport and delivery to other organs and

storage sites (e.g. see studies by Black & Skinner, 1986, and by Salmerón, 2018, in rainbow trout *Oncorhynchus mykiss* and a review of several fish species – including zebrafish *Danio rerio*, Salmoniformes and Perciformes, respectively). Therefore, it is expected that as lipids are mobilized from liver to supply energetic needs of different tissues as juvenile fish grow, the FA profile in liver will vary with time. Moreover, the regulation of lipid mobilization throughout time depends on various hormones that act as adipokinetic agents (Sheridan, 1988) and modulate endogenous lipogenesis and lipolysis (e.g. insulin, growth factors, cortisol and sex hormones, Weil et al., 2013). In turn, hormones can be affected by several internal or external factors. Given that water parameters (except for temperature in this study, which did not affect FA profiles), as well as feed supplied to animals during the experiments were the same for all animals at all times, it is likely that other factors affecting hormones were at play, including intrinsic ones such as developmental stage and sexual maturity (Leaf et al., 2018; Li et al., 2018). In our experimental trials, each tank contained several fish in typical dominance-based social groups. Dominance is a key determinant of development and maturation in this fish species (Khoo et al., 2018; Mitchell and Dill, 2005), as there is usually a dominant fish pair that reaches sexual maturity and smaller non-breeding fish within each social group. Although we did not assess developmental status throughout the experiment, we suggest that temporal lipid dynamics may have been affected as social relationships between fish changed throughout the experiment. For instance, after each sampling time point, when some fish were removed from tanks and euthanized for analyses, rearrangements in social dominance may have occurred. Social dominance not only affects growth and maturation of fish through hormonal changes, but could also influence the food intake of the smaller fish which are lower in hierarchy, leading to oscillations in lipid accumulation and mobilization and, consequently, FA profile over time.

5. Conclusions

Overall, current increases in tropical ocean temperatures do not affect *A. ocellaris* lipid contents, fatty acid profile and lipid metabolism or weight, suggesting that stable lipid signatures may be an adaptive feature of thermal tolerant juvenile fish stages, as also recently suggested for marine invertebrate species (e.g. marine annelids, Madeira et al. 2021). By maintaining overall energetic balance at higher temperature, these organisms may persist during the expansion of ocean warm pools, at least in the short term. Whether the thermal tolerance found in this study will allow long-term persistence of the species in the environment under temperature regime changes will however ultimately depend on other interactive factors, such as i) *A. ocellaris* life-stage specific vulnerability and capacity for adaption on evolutionary timeframes; ii) habitat suitability, as coral reefs have already been severely affected at 30 °C in past years, see Hoegh-Guldberg et al., 2017 for a review); iii) clownfish host anemone survival under climate change, as there have reports of anemone mortality or reduction in size during bleaching events, with detrimental effects on anemonefish populations, including reduced social group sizes, decreased dominant fish length, and reduced fecundity and recruitment, namely in *Amphiprion* spp. (Mitchell and Dill, 2005; Saenz-Agudelo et al., 2011; Beldade et al., 2017); and iv) plankton nutrition quality and availability, coupled to foraging efficiency of ocellaris clownfish in warming oceans (Nowicki et al., 2012).

We also conclude that FA profile differences between muscles and liver coupled to specific enhanced lipid metabolic pathways in liver, namely α -linolenic and linoleic acid metabolism, indicate that liver plays an important role in maintaining homeostasis during environmentally challenging situations, through the production of lipid-derived metabolites that drive stress responses and/or acclimation. Additionally, temporal changes detected in FA profiles, mainly in liver, may be a result of growth processes that modulate organism lipid metabolism through time.

Finally, we conclude that the influence of future oceans in organisms' lipid signatures may be difficult to predict, as species-, population- or even life-stage-specific mechanisms seem

to regulate energy and lipid homeostasis. Particularly, we highlight the need for research comparing climate change effects on lipid metabolic networks and plasticity mechanisms between wild populations from different areas of the distribution range, or among species along natural thermal gradients, to infer selection gradients that influence energy-limited tolerance to stress. Translocation experiments would also be useful to test the influence of local adaption on lipid responses to environmental change.

For now, it seems plausible to expect that changes in individuals' FA profiles and composition may be less affected when compared to overall changes in lipid availability in ecosystems as consequence of shifts in taxonomic structure of communities and biodiversity reorganization with climate change.

References

- Akhtar, M.S., Pal, A.K., Sahu, N.P., Ciji, A., Mahanta, P.C., 2014. Higher acclimation temperature modulates the composition of muscle fatty acid of *Tor putitora* juveniles. *Weather Clim. Extrem.* 4, 19–21. <https://doi.org/10.1016/j.wace.2014.03.001>
- Allen, G., 2009. *Field Guide To Marine Fishes of Tropical Australia and South East Asia*, 4th ed. Western Australian Museum.
- Anacleto, P., Maulvault, A.L., Bandarra, N.M., Repolho, T., Nunes, M.L., Rosa, R., Marques, A., 2014. Effect of warming on protein, glycogen and fatty acid content of native and invasive clams. *Food Res. Int.* 64, 439–445. <https://doi.org/10.1016/j.foodres.2014.07.023>
- Angilletta, M.J., Wilson, R.S., Navas, C.A., James, R.S., 2003. Tradeoffs and the evolution of thermal reaction norms. *Trends Ecol. Evol.* 18, 234–240. [https://doi.org/10.1016/S0169-5347\(03\)00087-9](https://doi.org/10.1016/S0169-5347(03)00087-9)
- Arora, A., Rao, S.A., Chattopadhyay, R., Goswami, T., George, G., Sabeerali, C.T., 2016. Role of Indian Ocean SST variability on the recent global warming hiatus. *Glob. Planet. Change* 143, 21–30. <https://doi.org/10.1016/j.gloplacha.2016.05.009>

Ayala, A., Muñoz, M.F., Argüelles, S., 2014. Lipid peroxidation: production, metabolism and signaling mechanisms of malondialdehyde and 4-hydroxy-2-nonenal. *Oxid. Med. Cell. Longev.* 2014, Article ID 360438, 31 pages. <https://doi.org/10.1093/europace/eux022>

Balogh, G., Péter, M., Glatz, A., Gombos, I., Török, Z., Horváth, I., Harwood, J.L., Vígh, L., 2013. Key role of lipids in heat stress management. *FEBS Lett.* 587, 1970–1980. <https://doi.org/10.1016/j.febslet.2013.05.016>

Barbosa, V., Maulvault, A.L., Alves, R.N., Anacleto, P., Pousão-Ferreira, P., Carvalho, M.L., Nunes, M.L., Rosa, R., Marques, A., 2017. Will seabass (*Dicentrarchus labrax*) quality change in a warmer ocean? *Food Res. Int.* 97, 27–36. <https://doi.org/10.1016/j.foodres.2017.03.024>

Beldade, R., Blandin, A., O'Donnell, R., Mills, S.C., 2017. Cascading effects of thermally-induced anemone bleaching on associated anemonefish hormonal stress response and reproduction. *Nat. Commun.* 8, 716, <https://doi.org/10.1038/s41467-017-00565-w>

Bijma, J., Pörtner, H.O., Yesson, C., Rogers, A.D., 2013. Climate change and the oceans - What does the future hold? *Mar. Pollut. Bull.* 74, 495–505. <https://doi.org/10.1016/j.marpolbul.2013.07.022>

Black, D., Skinner, E.R., 1986. Features of the lipid transport system of fish as demonstrated by studies on starvation in the rainbow trout. *J. Comp. Physiol. B* 156, 497–502. <https://doi.org/10.1007/BF00691035>

Bobe, J., 2015. Egg quality in fish: Present and future challenges. *Anim. Front.* 5, 66–72. <https://doi.org/10.2527/af.2015-0010>

Boglino, A., Gisbert, E., Darias, M.J., Estévez, A., Andree, K.B., Sarasquete, C., Ortiz-delgado, J.B., 2012. Isolipidic diets differing in their essential fatty acid profiles affect the deposition of unsaturated neutral lipids in the intestine, liver and vascular system of Senegalese sole larvae and early juveniles. *Comp. Biochem. Physiol. Part A* 162, 59–70. <https://doi.org/10.1016/j.cbpa.2012.02.013>

Bouaziz, M., Bejaoui, S., Rabeh, I., Besbes, R., El, M.H., Falcon, J., 2017. Impact of temperature on sea bass, *Dicentrarchus labrax*, retina: Fatty acid composition, expression of rhodopsin and enzymes of lipid and melatonin metabolism. *Exp. Eye*

832 Res. 159, 87–97. <https://doi.org/10.1016/j.exer.2017.03.010>

833 Braekkan, O.R., 1959. A Comparative Study of Vitamins in the Trunk Muscles of Fishes,
834 Fiskeridirektoratets skrifter / Serie Teknologiske undersøkelser.

835 Bruneel, S., Gobeyn, S., Verhelst, P., Reubens, J., Moens, T., Goethals, P., 2018.
836 Implications of movement for species distribution models - Rethinking environmental
837 data tools. Sci. Total Environ. 628–629, 893–905.
838 <https://doi.org/10.1016/j.scitotenv.2018.02.026>

839 Calder, P.C., 2012. 5th International Immunonutrition Workshop Fatty acids Long-chain
840 fatty acids and inflammation. Proc. Nutr. Soc. 71, 284–289.
841 <https://doi.org/10.1017/S0029665112000067>

842 Calder, P.C., 2011. Fatty acids and inflammation: The cutting edge between food and
843 pharma. Eur. J. Pharmacol. 668, S50–S58.
844 <https://doi.org/10.1016/j.ejphar.2011.05.085>

845 Calder, P.C., 2010. Omega-3 Fatty Acids and Inflammatory Processes. Nutrients 2, 355–
846 374. <https://doi.org/10.3390/nu2030355>

847 Checa, A., Bedia, C., Jaumot, J., 2015. Lipidomic data analysis: Tutorial, practical
848 guidelines and applications. Anal. Chim. Acta 885, 1–16.
849 <https://doi.org/10.1016/j.aca.2015.02.068>

850 Chong, J., Wishart, D.S., Xia, J., 2019. Using MetaboAnalyst 4.0 for Comprehensive and
851 Integrative Metabolomics Data Analysis. Curr. Protoc. Bioinforma. 68, 1–128.
852 <https://doi.org/10.1002/cpbi.86>

853 Christen, F., Dufresne, F., Leduc, G., Dupont-cyr, B.A., Vandenberg, G.W., François, N.R.
854 Le, Tardif, J., Lamarre, S.G., Blier, P.U., 2020. Thermal tolerance and fish heart
855 integrity: fatty acids profiles as predictors of species resilience. Conserv. Physiol. 8,
856 coaa108. <https://doi.org/10.1093/conphys/coaa108>

857 Coleman, M.A., Butcherine, P., Kelaheer, B.P., Broadhurst, M.K., March, D.T., Provost, E.J.,
858 David, J., Benkendorff, K., 2019. Climate change does not affect the seafood quality
859 of a commonly targeted fish. Glob. Chang. Biol. 25, 699–707.
860 <https://doi.org/10.1111/gcb.14513>

Colombo, S.M., Rodgers, T.F.M., Diamond, M.L., Bazinet, R.P., Arts, M.T., 2019. Projected declines in global DHA availability for human consumption as a result of global warming. *Ambio* 49, 865–880. <https://doi.org/10.1007/s13280-019-01234-6>

Csoboz, B., Balogh, G.E., Kusz, E., Gombos, I., Peter, M., Crul, T., Gungor, B., Haracska, L., Bogdanovics, G., Torok, Z., 2013. Membrane fluidity matters: Hyperthermia from the aspects of lipids and membranes. *Int. J. Hyperth.* 29, 491–499. <https://doi.org/10.3109/02656736.2013.808765>

Dahlke, F.T., Wohlrab, S., Butzin, M., Pörtner, H.O., 2020. Thermal bottlenecks in the life cycle define climate vulnerability of fish. *Science* 369, 65–70. <https://doi.org/10.1126/science.aaz3658>

Dey, I., Buda, C., Wiik, T., Halver, J.E., Farkas, T., 1993. Molecular and structural composition of phospholipid membranes in livers of marine and freshwater fish in relation to temperature. *Proc. Natl. Acad. Sci. U.S.A.* 90, 7498–7502. <https://doi.org/10.1073/pnas.90.16.7498>

Eghetesadi-Araghi, P., Bastami, K.B., 2011. An integrated approach to interconnected effects between selected environmental parameters and fatty acid composition in mollusks. *Res. J. Environ. Sci.* 5, 310–315. <https://doi.org/10.3923/rjes.2011.310.315>

Ernst, R., Ejasing, C.S., Antonny, B., 2016. Homeoviscous Adaptation and the Regulation of Membrane Lipids. *J. Mol. Biol.* 428, 4776–4791. <https://doi.org/10.1016/j.jmb.2016.08.013>

Fahy, E., Sud, M., Cotter, D., Subramaniam, S., 2007. LIPID MAPS online tools for lipid research. *Nucleic Acids Res.* 35, 606–612. <https://doi.org/10.1093/nar/gkm324>

Fautin, D., Allen, G., 1992. Field Guide to Anemonefishes and their Host Sea Anemones. Perth: Western Australian Museum, Perth, Australia.

Frolkis, A., Knox, C., Lim, E., Jewison, T., Law, V., Hau, D.D., Liu, P., Gautam, B., Ly, S., Guo, A.C., Xia, J., Liang, Y., Shrivastava, S., Wishart, D.S., 2009. SMPDB: The small molecule pathway database. *Nucleic Acids Res.* 38, 480–487. <https://doi.org/10.1093/nar/gkp1002>

German, J.B., 1998. Fatty acids (dietary) and the immune system, *Nutr. Rev.* 56, S70–S83.

<https://doi.org/10.1111/j.1753-4887.1998.tb01648.x>

- Graham, N.A.J., McClanahan, T.R., MacNeil, M.A., Wilson, S.K., Polunin, N.V.C., Jennings, S., Chabanet, P., Clark, S., Spalding, M.D., Letourneur, Y., Bigot, L., Galzin, R., Öhman, M.C., Garpe, K.C., Edwards, A.J., Sheppard, C.R.C., 2008. Climate warming, marine protected areas and the ocean-scale integrity of coral reef ecosystems. *PLoS One* 3, e3039. <https://doi.org/10.1371/journal.pone.0003039>
- Groom, M.J., Meffe, G.K., Carroll, C.R., 2012. *Principles of Conservation Biology*, 3rd ed. Sinauer Associates, Inc. Sunderland, Massachusetts, USA. <https://doi.org/doi:10.17226/4919>
- Guil-Guerrero, L., Venegas-Venegas, E., Rincón-Cervera, M.A., Suárez, M.D., 2011. Fatty acid profiles of livers from selected marine fish species. *J. Food Compos. Anal.* 24, 217–222. <https://doi.org/10.1016/j.jfca.2010.07.011>
- Haliloğlu, H.İ., Bayir, A., Sirkecioğlu, A.N., Aras, N.M., 2011. Fatty Acid Profiles of Different Tissues in Mature Trout (*Salmo trutta macrostigma*) from Pulur Creek in Karasu Region, *J. Appl. Anim. Res.* 27, 81–84. <https://doi.org/10.1080/09712119.2005.9706545>
- Herbert, T.D., Peterson, L.C., Lawrence, K.T., Liu, Z., 2010. Tropical Ocean Temperatures Over the Past 3.5 Million Years. *Science* 328, 1530–1534. <https://doi.org/10.1126/science.1185435>
- Hernando, M., Schloss, I.R., Almandoz, G.O., Malanga, G., Varela, D.E., Troch, M. De, 2018. Combined effects of temperature and salinity on fatty acid content and lipid damage in Antarctic phytoplankton. *J. Exp. Mar. Bio. Ecol.* 503, 120–128. <https://doi.org/10.1016/j.jembe.2018.03.004>
- Hixson, S.M., Arts, M.T., 2016. Climate warming is predicted to reduce omega-3, long-chain, polyunsaturated fatty acid production in phytoplankton. *Glob. Change Biol.* 22, 2744–2755. <https://doi.org/10.1111/gcb.13295>
- Hocquette, J.F., Gondret, F., Baéza, E., Médale, F., Jurie, C., Pethick, D.W., 2010. Intramuscular fat content in meat-producing animals: development, genetic and nutritional control, and identification of putative markers. *Animal* 4, 303–319.

919 <https://doi.org/10.1017/S1751731109991091>

920 Hoegh-Guldberg, O., Poloczanska, E.S., Skirving, W., Dove, S., 2017. Coral reef
 921 ecosystems under climate change and ocean acidification. *Front. Mar. Sci.* 4, 158.
 922 <https://doi.org/10.3389/fmars.2017.00158>

923 Horn, S.S., Ruyter, B., Meuwissen, T.H.E., Moghadam, H., Hillestad, B., Sonesson, A.K.,
 924 2020. GWAS identifies genetic variants associated with omega-3 fatty acid
 925 composition of Atlantic salmon fillets. *Aquaculture* 514, 734494.
 926 <https://doi.org/10.1016/j.aquaculture.2019.734494>

927 Howe, K., Clark, M.D., Torroja, C.F., Torrance, J., Berthelot, C., Muffato, M., Collins, J.E.,
 928 Humphray, S., McLaren, K., Matthews, L., et al. 2013. The zebrafish reference
 929 genome sequence and its relationship to the human genome. *Nature* 496, 498–503.
 930 <https://doi.org/10.1038/nature12111>

931 Innes, J.K., Calder, P.C., 2018. Omega-6 fatty acids and inflammation. *Prostaglandins*
 932 *Leukot. Essent. Fat. Acids* 132, 41–48. <https://doi.org/10.1016/j.plefa.2018.03.004>

933 IPCC, 2019. IPCC Special Report on the Ocean and Cryosphere in a Changing Climate
 934 [H.-O. Pörtner, D.C. Roberts, V. Masson-Delmotte, P. Zhai, M. Tignor, E.
 935 Poloczanska, K. Mintenbeck, A. Alegría, M. Nicolai, A. Okem, J. Petzold, B. Rama,
 936 N.M. Weyer (eds.)]. In press.

937 IPCC, 2014: Climate Change 2014: Synthesis Report. Contribution of Working Groups I, II
 938 and III to the Fifth Assessment Report of the Intergovernmental Panel on Climate
 939 Change [Core Writing Team, R.K. Pachauri and L.A. Meyer (eds.)]. IPCC, Geneva,
 940 Switzerland, 151 pp. <https://doi.org/10.1017/CBO9781107415324.004>

941 IPCC, 2013. Atlas of Global and Regional Climate Projections. *Clim. Chang.* 2013 Phys.
 942 Sci. Basis. Contrib. Work. Gr. I to Fifth Assess. Rep. Intergov. Panel Clim. Chang.
 943 Annexe I, 1311–1394. <https://doi.org/10.1017/CBO9781107415324.029>

944 Jewison, T., Su, Y., Disfany, F.M., Liang, Y., Knox, C., Maclejewski, A., Poelzer, J., Huynh,
 945 J., Zhou, Y., Arndt, D., Djoumbou, Y., Liu, Y., Deng, L., Guo, A.C., Han, B., Pon, A.,
 946 Kanehisa, M., Furumichi, M., Tanabe, M., Sato, Y., Morishima, K., 2017. KEGG: New
 947 perspectives on genomes, pathways, diseases and drugs. *Nucleic Acids Res.* 45,

D353–D361. <https://doi.org/10.1093/nar/gkw1092>

Khoo, M.L., Das, S.K., Ghaffar, M.A., 2018. Growth pattern, diet and reproductive biology of the clownfish *Amphiprion ocellaris* in waters of Pulau Tioman, Malaysia. Egypt. J.

Aquat. Res. 44, 233–239. <https://doi.org/10.1016/j.ejar.2018.07.003>

Klepsatel, P., Gálíková, M., Xu, Y., Kühnlein, R.P., 2016. Thermal stress depletes energy reserves in *Drosophila*. Sci. Rep. 6, 33667. <https://doi.org/10.1038/srep33667>

Kokla, M., Virtanen, J., Kolehmainen, M., Paananen, J., Hanhineva, K., 2019. Random forest-based imputation outperforms other methods for imputing LC-MS metabolomics data: A comparative study. BMC Bioinformatics 20, 1–11. <https://doi.org/10.1186/s12859-019-3110-0>

Leaf, R.T., Trushenski, J., Brown-Peterson, N.J., Andres, M.J., 2018. Temporal dynamics of lipid and fatty acid characteristics of Gulf Menhaden, *Brevoortia patronus*, in the northern Gulf of Mexico. Reg. Stud. Mar. Sci. 24, 1–9. <https://doi.org/10.1016/j.rsma.2018.06.011>

Lesser, M.P., 2006. Oxidative Stress in Marine Environments: Biochemistry and Physiological Ecology. Annu. Rev. Physiol. 68, 253–278. <https://doi.org/10.1146/annurev.physiol.68.040104.110001>

Li, S., Wen, W., Gong, X., Huang, X., Chen, N., 2018. Variation of lipids and fatty acids composition in the tissues of wild devil stinger (*Inimicus japonicas*) during sexual maturation. Aquac. Fish. 3, 115–121. <https://doi.org/10.1016/j.aaf.2018.05.004>

Lin, C.Y., Ho, C.R., Zheng, Q., Kuo, N.J., Chang, P., 2011. Warm pool variability and heat flux change in the global oceans. Glob. Planet. Change 77, 26–33. <https://doi.org/10.1016/j.gloplacha.2011.02.006>

Liu, C., Ge, J., Zhou, Y., Thirumurugan, R., Gao, Q., 2020. Effects of decreasing temperature on phospholipid fatty acid composition of different tissues and hematology in Atlantic salmon (*Salmo salar*). Aquaculture 515, 734587. <https://doi.org/10.1016/j.aquaculture.2019.734587>

Ma, J., Shojaie, A., Michailidis, G., 2019. A comparative study of topology-based pathway enrichment analysis methods. BMC Bioinformatics 20, 1–14.

977 <https://doi.org/10.1186/s12859-019-3146-1>
 978 Madeira, C., Madeira, D., Diniz, M.S., Cabral, H.N., Vinagre, C., 2017. Comparing
 979 biomarker responses during thermal acclimation: A lethal vs non-lethal approach in a
 980 tropical reef clownfish. *Comp. Biochem. Physiol. Part A Mol. Integr. Physiol.* 204, 104–
 981 112. <https://doi.org/10.1016/j.cbpa.2016.11.018>
 982 Madeira, C., Madeira, D., Diniz, M.S., Cabral, H.N., Vinagre, C., 2016. Thermal acclimation
 983 in clownfish: An integrated biomarker response and multi-tissue experimental
 984 approach. *Ecol. Indic.* 71, 280–292. <https://doi.org/10.1016/j.ecolind.2016.07.009>
 985 Madeira, C., Mendonça, V., Flores, A.A.V., Diniz, M.S., Vinagre, C., 2018. High thermal
 986 tolerance does not protect from chronic warming – A multiple end-point approach
 987 using a tropical gastropod, *Stramonita haemastoma*. *Ecol. Indic.* 91, 626–635.
 988 <https://doi.org/10.1016/j.ecolind.2018.04.044>
 989 Madeira, D., Madeira, C., Costa, P.M., Vinagre, C., Pörtner, H.O., Diniz, M.S., 2020.
 990 Different sensitivity to heatwaves across the life cycle of fish reflects phenotypic
 991 adaptation to environmental niche. *Mar. Environ. Res.* 162, 105192.
 992 <https://doi.org/10.1016/j.marenvres.2020.105192>
 993 Madeira, D., Fernandes, J.F., Jerónimo, D., Ricardo, F., Santos, A., Domingues, M.R.,
 994 Calado, R., 2021. Calcium homeostasis and stable fatty acid composition underpin
 995 heatwave tolerance of the keystone polychaete *Hediste diversicolor*. *Environ. Res.*
 996 195, 110885. <https://doi.org/https://doi.org/10.1016/j.envres.2021.110885>
 997 Miller, G.M., Kroon, F.J., Metcalfe, S., Munday, P.L., 2015. Temperature is the evil twin:
 998 Effects of increased temperature and ocean acidification on reproduction in a reef fish.
 999 *Ecol. Appl.* 25, 603–620. <https://doi.org/10.1594/PANGAEA.836664>
 1000 Mitchell, J.S., Dill, L.M., 2005. Why is group size correlated with the size of the host sea
 1001 anemone in the false clown anemonefish? *Can. J. Zool.* 83, 372–376.
 1002 <https://doi.org/10.1139/z05-014>
 1003 Morales, P.E., Bucarey, J.L., Espinosa, A., 2017. Muscle Lipid Metabolism: Role of Lipid
 1004 Droplets and Perilipins. *J. Diab. Res.* 2017, 1789395
 1005 <https://doi.org/10.1155/2017/1789395>

- Munday, P.L., McCormick, M.I., Nilsson, G.E., 2012. Impact of global warming and rising CO₂ levels on coral reef fishes: what hope for the future? *J. Exp. Biol.* 215, 3865–3873. <https://doi.org/10.1242/jeb.074765>
- Munro, D., Blier, P.U., 2012. The extreme longevity of *Arctica islandica* is associated with increased peroxidation resistance in mitochondrial membranes. *Aging Cell* 11, 845–855. <https://doi.org/10.1111/j.1474-9726.2012.00847.x>
- Neidleman, S.L., 1987. Effects of Temperature on Lipid Unsaturation Effects of Temperature on Lipid Unsaturation. *Biotechnol. Genet. Engineering Rev.* 5, 245–268. <https://doi.org/10.1080/02648725.1987.10647839>
- Nowicki, J.P., Miller, G.M., Munday, P.L., 2012. Interactive effects of elevated temperature and CO₂ on foraging behavior of juvenile coral reef fish. *J. Exp. Mar. Bio. Ecol.* 412, 46–51. <https://doi.org/10.1016/j.jembe.2011.10.020>
- Okazaki, Y., Saito, K., 2014. Roles of lipids as signaling molecules and mitigators during stress response in plants. *Plant J.* 79, 584–596. <https://doi.org/10.1111/tpj.12556>
- Pankhurst, N.W., Munday, P.L., 2011. Effects of climate change on fish reproduction and early life history stages. *Mar. Freshw. Res.* 62, 1015–1026. <https://doi.org/10.1071/MF10269>
- Parrish, C.C., 2013. Lipids in Marine Ecosystems. *ISRN Oceanogr.* 2013, 1–16.
- Payne, N.L., Smith, J.A., van der Meulen, D.E., Taylor, M.D., Watanabe, Y.Y., Takahashi, A., Marzullo, T.A., Gray, C.A., Cadiou, G., Suthers, I.M., 2016. Temperature dependence of fish performance in the wild: Links with species biogeography and physiological thermal tolerance. *Funct. Ecol.* 903–912. <https://doi.org/10.1111/1365-2435.12618>
- Pethybridge, H.R., Parrish, C.C., Morrongiello, J., Young, J.W., Farley, J.H., Gunasekera, R.M., Nichols, P.D., 2015. Spatial patterns and temperature predictions of tuna fatty acids: Tracing essential nutrients and changes in primary producers. *PLoS One* 10, 1–17. <https://doi.org/10.1371/journal.pone.0131598>
- Petitjean, Q., Jean, S., Gandar, A., Côte, J., Laffaille, P., Jacquin, L., 2019. Stress responses in fish: From molecular to evolutionary processes. *Sci. Total Environ.* 684,

371–380. <https://doi.org/10.1016/j.scitotenv.2019.05.357>

Pörtner, H.O., Mark, F.C., Bock, C., 2004. Oxygen limited thermal tolerance in fish? Answers obtained by nuclear magnetic resonance techniques, *Respirat. Physiol. Neurobiol* 141, 243–260. <https://doi.org/10.1016/j.resp.2004.03.011>

Rainuzzo, J.R., Reitan, K.I., Olsen, Y., 1997. The significance of lipids at early stages of marine fish: a review. *Aquaculture* 155, 103–115. [https://doi.org/10.1016/S0044-8486\(97\)00121-X](https://doi.org/10.1016/S0044-8486(97)00121-X)

Roessig, J., Woodley, C., 2004. Effects of global climate change on marine and estuarine fishes and fisheries. *Rev. Fish Biol. Fish.* 14, 251–275. <https://doi.org/10.1007/s11160-004-6749-0>

Roux, N., Salis, P., Lambert, A., Logeux, V., Soulat, O., Romans, P., Frédérick, B., Lecchini, D., Laudet, V., 2019. Staging and normal table of postembryonic development of the clownfish (*Amphiprion ocellaris*). *Dev. Dyn.* 248, 545–568. <https://doi.org/10.1002/dvdy.46>

Rummer, J.L., Couturier, C.S., Stecyk, J.A.W., Gardiner, N.M., Kinch, J.P., Nilsson, G.E., Munday, P.L., 2014. Life on the edge: Thermal optima for aerobic scope of equatorial reef fishes are close to current day temperatures. *Glob. Chang. Biol.* 20, 1055–1066. <https://doi.org/10.1111/gcb.12455>

Rushworth, K.J.W., Smith, S.D.A., Cowden, K.L., Purcell, S.W., 2011. Optimal temperature for growth and condition of an endemic subtropical anemonefish. *Aquaculture* 318, 479–482. <https://doi.org/10.1016/j.aquaculture.2011.06.004>

Ruyter, B., Moya-Falcón, C., Rosenlund, G., Vegusdal, A., 2006. Fat content and morphology of liver and intestine of Atlantic salmon (*Salmo salar*): Effects of temperature and dietary soybean oil. *Aquaculture* 252, 441–452. <https://doi.org/10.1016/j.aquaculture.2005.07.014>

Saenz-Agudelo, P., Jones, G.P., Thorrold, S.R., Planes, S., 2011. Detrimental effects of host anemone bleaching on anemonefish populations. *Coral Reefs* 30, 497–506. <https://doi.org/10.1007/s00338-010-0716-0>

1064 Salmerón, C., 2018. Adipogenesis in fish. J. Exp. Biol. 121, jeb161588.
 1065 <https://doi.org/10.1242/jeb.161588>

1066 Salway, J.G., 2013. Metabolism at a glance. 3rd edition, Alden, Mass.: Wiley-Blackwell
 1067 Pub.

1068 Sargent, J.R., Mcevoy, L.A., Bell, J.G., 1997. Requirements, presentation and sources of
 1069 polyunsaturated fatty acids in marine fish larval feeds. Aquaculture 155, 117–127.
 1070 [https://doi.org/10.1016/S0044-8486\(97\)00122-1](https://doi.org/10.1016/S0044-8486(97)00122-1)

1071 Sheridan, M.A., 1988. Lipid dynamics in fish: aspects of absorption, transportation,
 1072 deposition and mobilization. Comp. Biochem. Physiol. - Part B Biochem. 90, 679–690.
 1073 [https://doi.org/10.1016/0305-0491\(88\)90322-7](https://doi.org/10.1016/0305-0491(88)90322-7)

1074 Sidell, B.D., Crockett, E.L., Driedzic, W.R., 1995. Antarctic fish tissues preferentially
 1075 catabolize monoenoic fatty acids. J. Exp. Zool. 271, 73–81.
 1076 <https://doi.org/10.1002/jez.1402710202>

1077 Sinensky, M., 1974. Homeoviscous Adaptation - A Homeostatic Process that Regulates the
 1078 Viscosity of Membrane Lipids in *Escherichia coli*. Proc. Natl. Acad. Sci. USA 71, 522–
 1079 525. <https://doi.org/10.1073/pnas.71.2.522>

1080 Sokolova, I.M., 2013. Energy-limited tolerance to stress as a conceptual framework to
 1081 integrate the effects of multiple stressors. Integr. Comp. Biol. 53, 597–608.
 1082 <https://doi.org/10.1093/icb/ict028>

1083 Sun, Z., Tan, X., Liu, Q., Ye, H., Zou, C., Xu, M., Zhang, Y., Ye, C., 2019. Physiological,
 1084 immune responses and liver lipid metabolism of orange-spotted grouper (*Epinephelus*
 1085 *coioides*) under cold stress. Aquaculture 498, 545–555.
 1086 <https://doi.org/10.1016/j.aquaculture.2018.08.051>

1087 Todd, C.D., Hughes, S.L., Marshall, C.T., MacLean, J.C., Lonergan, M.E., Biuw, E.M.,
 1088 2008. Detrimental effects of recent ocean surface warming on growth condition of
 1089 Atlantic salmon. Glob. Chang. Biol. 14, 958–970. [https://doi.org/10.1111/j.1365-](https://doi.org/10.1111/j.1365-2486.2007.01522.x)
 1090 [2486.2007.01522.x](https://doi.org/10.1111/j.1365-2486.2007.01522.x)

1091 Török, Z., Crul, T., Maresca, B., Schütz, G.J., Viana, F., Dindia, L., Piotto, S.,
 1092 Brameshuber, M., Balogh, G., Péter, M., Porta, A., Trapani, A., Gombos, I., Glatz, A.,

1093 Gungor, B., Peksel, B., Vigh, L., Csoboz, B., Horváth, I., Vijayan, M.M., Hooper, P.L.,
 1094 Harwood, J.L., Vigh, L., 2014. Plasma membranes as heat stress sensors: From lipid-
 1095 controlled molecular switches to therapeutic applications. *BBA - Biomembr.* 1838,
 1096 1594–1618. <https://doi.org/10.1016/j.bbamem.2013.12.015>
 1097 Uchiyama, M., Mihara, M., 1978. Determination of malonaldehyde precursor in tissues by
 1098 thiobarbituric acid test. *Anal. Biochem.* 86, 271–278. [https://doi.org/10.1016/0003-](https://doi.org/10.1016/0003-2697(78)90342-1)
 1099 [2697\(78\)90342-1](https://doi.org/10.1016/0003-2697(78)90342-1)
 1100 Valles-Regino, R., Tate, R., Kelaher, B., Savins, D., Dowell, A., Benkendorff, K., 2015.
 1101 Ocean Warming and CO₂-Induced Acidification Impact the Lipid Content of a Marine
 1102 Predatory Gastropod. *Mar. Drugs* 13, 6019–6037.
 1103 <https://doi.org/10.3390/md13106019>
 1104 Vannice, G., Rasmussen, H., 2014. Position of the academy of nutrition and dietetics:
 1105 Dietary fatty acids for healthy adults. *J. Acad. Nutr. Diet.* 114, 136–153.
 1106 <https://doi.org/10.1016/j.jand.2013.11.001>
 1107 Vargas, A., Piccinetti, C.C., Carnevali, O., Chemello, G., Randazzo, B., Olivotto, I., 2016.
 1108 Marine ornamental species culture: From the past to “Finding Dory.” *Gen. Comp.*
 1109 *Endocrinol.* 245, 116–121. <https://doi.org/10.1016/j.ygcen.2016.03.004>
 1110 Wei, R., Wang, J., Su, M., Jia, E., Chen, S., Chen, T., 2018. Missing Value Imputation
 1111 Approach for Mass Spectrometry-based Metabolomics Data. *Sci. Rep.* 1–10.
 1112 <https://doi.org/10.1038/s41598-017-19120-0>
 1113 Weil, C., Lefèvre, F., Bugeon, J., 2013. Characteristics and metabolism of different adipose
 1114 tissues in fish, *Reviews in Fish Biology and Fisheries.* [https://doi.org/10.1007/s11160-](https://doi.org/10.1007/s11160-012-9288-0)
 1115 [012-9288-0](https://doi.org/10.1007/s11160-012-9288-0)
 1116 Wen, B., Jin, S.-R., Chen, Z.-Z., Gao, J.-Z., Wang, L., Liu, Y., Liu, H.-P., 2017. Plasticity of
 1117 energy reserves and metabolic performance of discus fish (*Symphysodon*
 1118 *aequifasciatus*) exposed to low-temperature stress. *Aquaculture* 481, 169–176.
 1119 <https://doi.org/10.1016/j.aquaculture.2017.09.002>
 1120 Wilson, M., Rafatnia, S., Liu, P., Wishart, D.S., 2014. SMPDB 2.0: Big improvements to the
 1121 small molecule pathway database. *Nucleic Acids Res.* 42, 478–484.

<https://doi.org/10.1093/nar/gkt1067>

Xia, J., Wishart, D.S., 2010. MetPA : a web-based metabolomics tool for pathway analysis and visualization 26, 2342–2344. <https://doi.org/10.1093/bioinformatics/btq418>

Züllig, T., Trötz Müller, M., Köfeler, H.C., 2020. Lipidomics from sample preparation to data analysis: a primer. Anal. Bioanal. Chem. 412, 2191–2209. <https://doi.org/10.1007/s00216-019-02241-y>

FIGURE CAPTIONS

Fig. 1 Fatty acid profiles of clownfish *Amphiprion ocellaris* subjected to 26 °C (n = 21 fish) and 30 °C (n = 17 fish). **(A)** PCA 2D score plot of FA profiles **(B)** heatmap of clustered FA classes; the colour scale ranges from red (higher than mean concentration) to blue (lower than mean concentration). Rows are the fatty acid classes and ratios, and columns are the mean of sample values. No significant differences were found in FA profiles between temperatures (PERMANOVA Pseudo-F = 0.910, p-value = 0.435).

Fig. 2 Fatty acid differences between muscle vs liver tissue, analysed in n = 38 clownfish. **(A)** PCA 2D score plot of FA profiles **(B)** heatmap of clustered FA classes; the colour scale ranges from red (higher than mean concentration) to blue (lower than mean concentration). Rows are the fatty acid classes and ratios, and columns are the mean of sample values. Significant differences were found in FA profiles between tissues (PERMANOVA Pseudo-F = 61.091, p-value < 0.001).

Fig. 3 Fatty acid differences between T0 vs T7 vs T14 vs T21 vs T28 sampling timepoints assessed in the clownfish *Amphiprion ocellaris* (n = 3-5 fish per time-point). **(A)** PCA 2D score plot of FA profiles **(B)** heatmap of clustered FA classes; the colour scale ranges from red (higher than mean concentration) to blue (lower than mean concentration). Rows are the fatty acid classes and ratios, and columns are the mean of sample values. Significant

differences were found in FA profiles between times (PERMANOVA Pseudo-F = 2.394, p-value = 0.004).

Fig. 4 Quantitative enrichment and pathway analysis of clownfish (*Amphiprion ocellaris*) fatty acid concentration comparing muscle vs liver tissues. **(A)** Metabolite set enrichment analysis showing significantly enriched pathways based on the group of 20 functionally related FA used as input data **(B)** pathway topology analysis, higher pathway relevance if impact > 0.1 and $-\log(p) > 8$ (for FDR < 0.05). All the matched pathways are displayed as circles and the colour and size of each circle are based on p-value and pathway impact value, respectively.

TABLES

Table 1. List of twenty-six fatty acids analyzed in this study. Abb: FA – fatty acids; SFA – saturated fatty acids; MUFA – mono-unsaturated fatty acids; PUFA – polyunsaturated fatty acids; HUFA – highly unsaturated fatty acids; NA – Not available; LMSD – Lipid Maps Structure Database; KEGG – Kyoto Encyclopedia of Genes and Genomes; HMDB – Human Metabolome Database.

Analytes (FA)	Common name	Formula	Class	Omega	LMSD ID	KEGG ID	HMDB ID	Retention time (min)
14:0	Myristic acid	C ₁₄ H ₂₈ O ₂	SFA	-	LMFA01010014	C06424	HMDB0000806	14.91
15:0	Pentadecylic acid	C ₁₅ H ₃₀ O ₂	SFA	-	LMFA01010015	C16537	HMDB0000826	17.29
16:1n-7	Cis-9-Palmitoleic acid	C ₁₆ H ₃₀ O ₂	MUFA	n-7	LMFA01030056	C08362	HMDB0003229	19.17
16:0	Palmitic acid	C ₁₆ H ₃₂ O ₂	SFA	-	LMFA01010001	C00249	HMDB0000220	19.71
17:1n-7	10Z-Heptadecenoic acid	C ₁₇ H ₃₂ O ₂	MUFA	n-7	LMFA01030283	C16536	HMDB0060038	21.52
17:0	Margaric acid	C ₁₇ H ₃₄ O ₂	SFA	-	LMFA01010017	NA	HMDB0002259	22.01
18:2n-6c	Linoleic acid	C ₁₈ H ₃₂ O ₂	PUFA	n-6	LMFA01030120	C01595	HMDB0000673	23.54
18:2n-6t	Linolelaidic acid	C ₁₈ H ₃₂ O ₂	PUFA	n-6	LMFA01030123	NA	HMDB0006270	23.72
18:1n-9c	Cis-Oleic acid	C ₁₈ H ₃₄ O ₂	MUFA	n-9	LMFA01030002	C00712	HMDB0000207	23.72
18:1n-9t	9-elaidic acid	C ₁₈ H ₃₄ O ₂	MUFA	n-9	LMFA01030073	C01712	HMDB0000573	23.85
18:0	Stearic acid	C ₁₈ H ₃₆ O ₂	SFA	-	LMFA01010018	C01530	HMDB0000827	24.30
19:1n-9	10Z-nonadecenoic acid	C ₁₉ H ₃₆ O ₂	MUFA	n-9	LMFA01030362	C00174	HMDB0013622	25.92
20:5n-3	Eicosapentaenoic acid (EPA)	C ₂₀ H ₃₀ O ₂	HUFA	n-3	LMFA01030759	C06428	HMDB0001999	27.11
20:4n-6	Arachidonic acid (ARA)	C ₂₀ H ₃₂ O ₂	HUFA	n-6	LMFA01030001	C00219	HMDB0001043	27.25
20:3n-3	11, 14, 17-eicosatrienoic acid	C ₂₀ H ₃₄ O ₂	PUFA	n-3	LMFA01030159	C16522	HMDB0060039	27.50
20:3n-6	8Z, 12E, 14Z-eicosatrienoic acid	C ₂₀ H ₃₄ O ₂	PUFA	n-6	LMFA01030388	C03442	HMDB0002925	27.50
20:1n-9	Cis-gondoic acid	C ₂₀ H ₃₈ O ₂	MUFA	n-9	LMFA01030085	C16526	HMDB0002231	28.05
20:0	Arachidic acid	C ₂₀ H ₄₀ O ₂	SFA	-	LMFA01010020	C06425	HMDB0002212	28.60
22:6n-3	Docosahexaenoic acid (DHA)	C ₂₂ H ₃₂ O ₂	HUFA	n-3	LMFA01030185	C06429	HMDB0002183	31.06
22:5n-3	Docosapentaenoic acid (DPA)	C ₂₂ H ₃₄ O ₂	HUFA	n-3	LMFA04000044	C16513	HMDB0006528	31.22

22:4n-6	Adrenic acid	C ₂₂ H ₃₆ O ₂	HUFA	n-6	LMFA01030178	C16527	HMDB0002226	31.35
22:2n-6	13Z,16Z-docosadienoic acid	C ₂₂ H ₄₀ O ₂	PUFA	n-6	LMFA01030405	C16533	HMDB0062219	32.00
22:0	Behenic acid	C ₂₂ H ₄₄ O ₂	SFA	-	LMFA01010022	C08281	HMDB0000944	32.60
24:1n-9	Nervonic acid	C ₂₄ H ₄₆ O ₂	MUFA	n-9	LMFA01030092	C08323	HMDB0002368	35.86
26:2n-6	17,20-hexacosadienoic acid	C ₂₆ H ₄₈ O ₂	PUFA	n-6	LMFA01030133	NA	NA	39.11
27:2	5Z,9Z-heptacosadienoic acid	C ₂₇ H ₅₀ O ₂	PUFA	NA	LMFA01020363	NA	NA	41.91

Table 2. Multivariate PERMANOVA results, testing the main effects of Temperature (26 °C vs 30 °C), Tissue (muscle vs liver) and Time (T0, T7, T14, T21, T28) as well as factor interactions on fatty acids concentration. Significant results are presented with an asterisk.

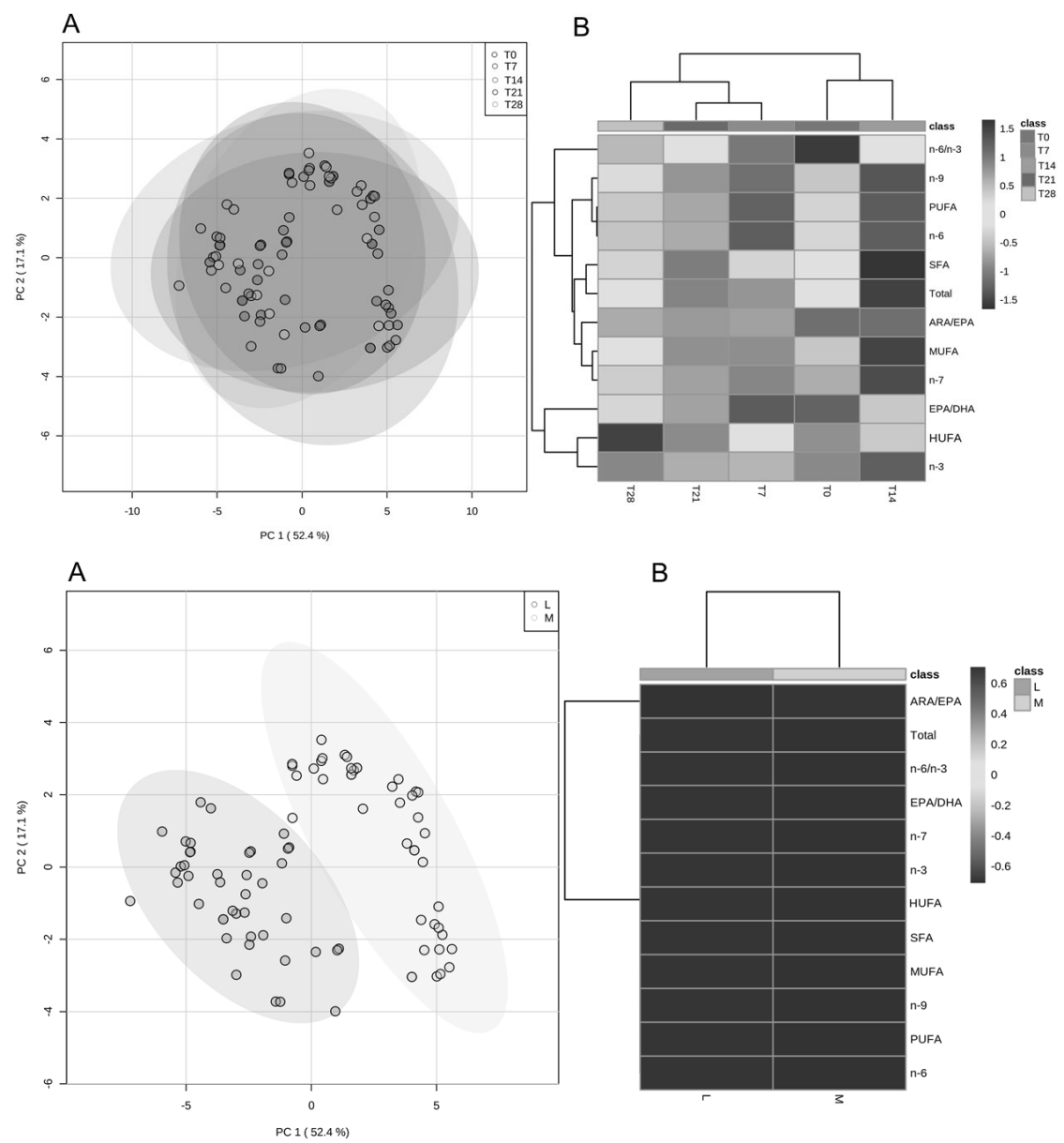
	<i>df</i>	<i>MS</i>	<i>Pseudo-F</i>	<i>P(perm)</i>	<i>perms</i>
Temperature	1	17.595	0.910	0.435	9935
Tissue	1	1181.300	61.091	<0.001*	9929
Time	4	46.287	2.394	0.004*	9916
Temperature × Tissue	1	19.527	1.010	0.372	9929
Temperature × Time	4	20.910	1.081	0.351	9921
Tissue × Time	4	38.008	1.966	0.017*	9919
Temperature × Tissue × Time	4	17.211	0.890	0.569	9903

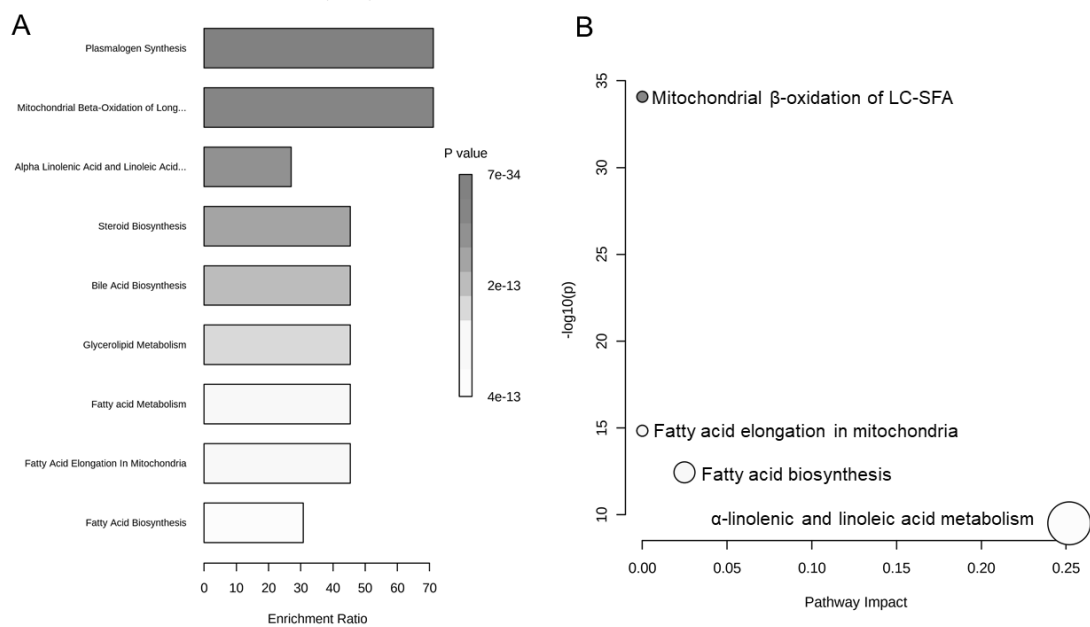
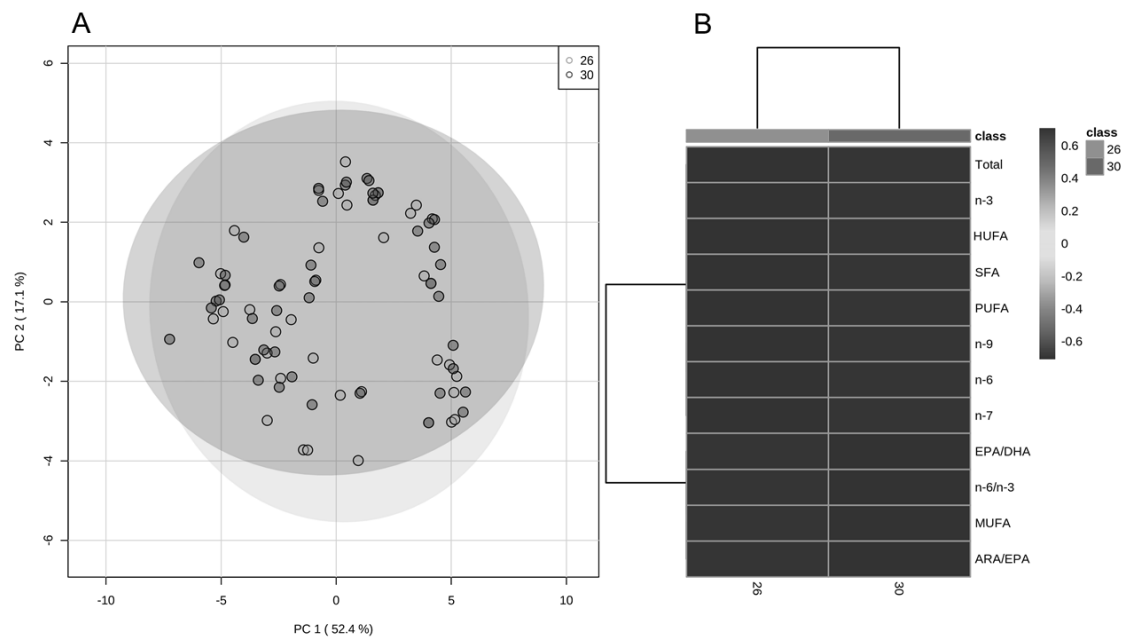
Table 3. Similarity of percentage analysis (SIMPER) of FA relative contribution to significant differences found among tissues and time groups (cutoff threshold at 90 % cumulative contribution).

Tissue		Time													
M vs. L		T7 vs. T14				T14 vs. T21				T14 vs. T28					
Fatty acid		Contribb%	Cum.%	Fatty acid		Contribb%	Cum.%	Fatty acid		Contribb%	Cum.%	Fatty acid		Contribb%	Cum.%
27:2		3.65	3.65	14:0		6.05	6.05	14:0		5.91	5.91	14:0		7.72	7.72
18:0		3.6	7.25	20:3n-3 + 20:3n-6		5.5	11.55	20:3n-3 + 20:3n-6		5.64	11.55	20:3n-3 + 20:3n-6		6.51	14.23
26:2n-6		3.5	10.75	16:1n-7		4.68	16.23	20:5n-3		4.98	16.52	16:1n-7		5.55	19.78
17:0		3.43	14.17	19:1n-9		4.62	20.85	18:2n-6t + 18:1n-9c		4.7	21.22	Σn-7		4.97	24.75
ΣSFA		3.39	17.56	Σn-3		4.57	25.41	19:1n-9		4.17	25.39	20:5n-3		4.25	29.01
ΣTotal		3.35	20.91	22:6n-3 (DHA)		4.47	29.89	20:4n-6 (ARA)		4.09	29.48	22:2n-6		3.98	32.99
18:1n-9t		3.31	24.22	Σn-7		4.28	34.17	15:0		4.09	33.57	19:1n-9		3.91	36.9
24:1n-9		3.3	27.52	ΣHUFA		4.21	38.38	22:6n-3 (DHA)		4.08	37.66	EPA/DHA		3.89	40.78
ΣPUFA		3.21	30.74	EPA/DHA		4.01	42.38	Σn-3		4.04	41.7	15:0		3.85	44.64
ΣMUFA		3.16	33.9	22:4n-6		3.9	46.28	16:1n-7		3.87	45.57	22:6n-3 (DHA)		3.83	48.47
ARA/EPA		3.13	37.03	20:5n-3		3.7	49.98	EPA/DHA		3.76	49.33	20:4n-6 (ARA)		3.73	52.2
Σn-9		3.05	40.08	20:4n-6 (ARA)		3.51	53.48	ΣHUFA		3.68	53.01	17:1n-7		3.6	55.81
17:1n-7		3.03	43.12	18:2n-6t + 18:1n-9c		3.43	56.91	Σn-7		3.54	56.55	20:0		3.55	59.36
16:0		2.99	46.11	17:1n-7		3.26	60.17	20:0		3.22	59.77	Σn-3		3.51	62.87
22:5n-3 (EPA)		2.87	48.98	22:2n-6		3.11	63.28	17:1n-7		3.03	62.8	ΣHUFA		3.46	66.32
Σn-6		2.86	51.84	22:0		3.02	66.3	22:4n-6		2.98	65.77	22:4n-6		3.41	69.74
Σn-6/Σn-3		2.84	54.68	15:0		3.01	69.31	22:0		2.62	68.39	18:2n-6t + 18:1n-9c		2.87	72.61
EPA/DHA		2.81	57.49	Σn-6		2.8	72.1	22:2n-6		2.44	70.83	ΣMUFA		2.35	74.96
20:1n-9		2.81	60.3	20:0		2.78	74.88	Σn-6		2.3	73.13	Σn-6		2.24	77.19
18:2n-6c		2.73	63.03	18:2n-6c		2.66	77.55	Σn-9		2.18	75.31	18:2n-6		2.14	79.33
Σn-7		2.69	65.72	22:5n-3 (EPA)		2.5	80.05	Σn-6/Σn-3		2.09	77.4	Σn-9		2.06	81.38
16:1n-7		2.59	68.31	ΣMUFA		2.23	82.27	20:1n-9		2.04	79.44	20:1n-9		2.05	83.43
22:0		2.54	70.85	20:1n-9		2.17	84.44	18:2n-6		2	81.44	Σn-6/Σn-3		1.98	85.42
18:2n-6t + 18:1n-9c		2.52	73.37	Σn-9		2.11	86.55	ΣMUFA		1.93	83.37	22:0		1.95	87.37
20:3n-3 + 20:3n-6		2.5	75.87	Σn-6/Σn-3		2.02	88.57	ARA/EPA		1.92	85.29	ARA/EPA		1.71	89.09

22:6n-3 (DHA)	2.39	78.26		16:0	1.87	87.17	
20:5n-3	2.35	80.61		ΣPUFA	1.62	88.79	
14:0	2.34	82.95					
15:0	2.26	85.21					
22:2n-6	2.23	87.44					
Σn-3	2.2	89.64					

FIGURES





SUPPLEMENTAL MATERIAL

Table S1. Fatty acid profile ($\mu\text{g}\cdot\text{mg}^{-1}$ dry tissue weight, mean \pm SD) of *A. ocellaris* muscle tissue at different temperature conditions (26 °C vs 30 °C) and timepoints (T0, T7, T14, T21, T28), N_{total} = 38 specimens.

MUSCLE	Overall control T0	26 °C					30 °C					Overall muscle
		T7					T28					
		T7	T14	T21	T28	Overall 26 °C	T7	T14	T21	T28	Overall 30 °C	
C14:0	0.96±0.79	0.96±0.77	0.60±0.42	0.24±0.02	0.74±0.43	0.74±0.65	0.62±0.87	1.11±1.16	0.30±0.13	0.85±0.36	0.78±0.75	0.76±0.66
C15:0	0.48±0.31	0.42±0.18	0.28±0.19	0.58±0.04	0.25±0.06	0.40±0.23	0.47±0.15	0.38±0.13	0.36±0.19	0.32±0.14	0.41±0.21	0.40±0.22
C16:1n7	1.69±1.16	1.55±1.37	1.42±0.61	0.27±0.08	1.42±0.72	1.35±1.07	0.93±0.87	1.95±1.38	0.87±0.75	1.47±0.77	1.40±1.13	1.38±1.10
C16:0	7.54±5.78	8.35±5.30	7.90±2.42	3.39±0.37	8.63±2.86	7.38±4.47	6.45±3.63	7.00±4.26	6.26±3.37	2.42±1.05	6.24±4.41	6.80±4.48
C17:1n7	0.30±0.15	0.43±0.38	0.27±0.09	0.14±0.01	0.28±0.12	0.30±0.23	0.21±0.11	0.38±0.17	0.19±0.09	0.29±0.10	0.28±0.15	0.29±0.19
C17:0	0.24±0.07	0.27±0.16	0.27±0.08	0.17±0.03	0.23±0.05	0.24±0.10	0.19±0.05	0.28±0.08	0.21±0.07	0.26±0.07	0.23±0.08	0.24±0.09
C18:2n6c	3.05±1.68	2.54±1.85	2.37±0.76	1.51±0.17	2.85±0.87	2.52±1.41	1.64±1.31	2.67±1.75	1.76±0.64	2.47±0.57	2.33±1.47	2.42±1.44
C18:2n6t + C18:1n9c ¹	5.93±3.06	3.38±2.75	4.81±1.89	2.82±0.69	5.61±1.67	4.57±2.59	3.99±2.30	6.25±3.70	4.07±1.82	5.75±2.27	5.20±2.95	4.89±2.80
C18:1n9t	1.94±0.98	1.61±1.16	1.41±0.59	0.61±0.06	1.74±0.67	1.52±0.93	1.18±0.73	1.94±1.22	1.33±0.95	1.44±0.58	1.59±1.00	1.55±0.97
C18:0	2.95±0.99	2.42±1.11	2.56±0.61	1.72±0.21	2.97±0.61	2.56±0.92	2.33±0.71	2.95±0.96	2.28±0.50	2.57±0.53	2.64±0.85	2.60±0.88
C19:1n9	0.27±0.14	0.41±0.17	0.22±0.14	0.41±0.08	0.23±0.02	0.30±0.15	0.29±0.14	0.23±0.10	0.28±0.09	0.28±0.19	0.27±0.13	0.28±0.15
C20:5n3	0.79±0.13	0.81±0.28	0.81±0.10	0.78±0.05	1.17±0.17	0.85±0.22	0.73±0.10	0.85±0.10	1.06±0.54	1.16±0.49	0.89±0.34	0.87±0.29
C20:4n6 (ARA)	1.48±0.28	1.58±0.48	1.21±0.31	1.01±0.11	1.76±0.51	1.41±0.44	1.25±0.33	1.31±0.30	1.56±0.51	1.23±0.38	1.37±0.38	1.39±0.41
C20:3n3 + C20:3n6 ²	0.41±0.20	0.45±0.35	0.44±0.16	0.23±0.01	0.57±0.18	0.42±0.24	0.25±0.16	0.72±0.42	0.38±0.20	0.55±0.19	0.46±0.31	0.44±0.28
C20:1n9	1.71±1.02	1.78±1.37	1.57±0.80	0.67±0.14	1.50±0.29	1.52±1.00	1.26±0.51	1.43±0.78	1.14±0.60	1.89±1.00	1.47±0.84	1.49±0.92
C20:0	0.36±0.32	0.46±0.25	0.26±0.18	0.37±0.17	0.17±0.03	0.33±0.25	0.25±0.20	0.24±0.13	0.23±0.14	0.41±0.32	0.29±0.24	0.31±0.24
C22:6n3 (DHA)	3.59±0.73	3.46±1.76	2.92±0.48	2.14±0.53	4.29±0.85	3.29±1.21	2.87±0.80	3.25±0.69	3.13±0.79	3.18±0.75	3.21±0.79	3.25±1.02

^{1,2} These FA have the same retention time and are eluted in a single merged peak in the GC.

C22:5n3 (EPA)	0.23±0.07	0.36±0.23	0.20±0.04	0.18±0.01	0.23±0.09	0.25±0.14	0.20±0.07	0.21±0.04	0.22±0.04	0.21±0.06	0.23±0.11
C22:4n6	1.17±0.45	1.16±0.78	0.77±0.29	0.45±0.05	1.63±0.82	1.03±0.66	0.75±0.35	0.82±0.38	1.11±0.45	0.97±0.45	1.00±0.56
C22:2n6	2.20±1.52	1.56±1.18	1.36±0.88	0.29±0.01	1.64±0.83	1.49±1.23	1.16±1.04	0.75±0.33	1.51±1.00	1.45±1.23	1.47±1.23
C22:0	0.28±0.23	0.39±0.30	0.18±0.06	0.20±0.05	0.17±0.00	0.26±0.21	0.15±0.02	0.15±0.03	0.16±0.02	0.18±0.13	0.22±0.17
C24:1n9	0.90±0.27	0.72±0.14	0.67±0.15	0.83±0.23	0.81±0.09	0.78±0.21	0.71±0.17	0.60±0.03	0.74±0.11	0.73±0.20	0.75±0.21
C26:2n6	1.44±0.13	1.42±0.14	1.47±0.20	1.91±0.51	1.65±0.39	1.54±0.32	1.63±0.25	1.50±0.19	1.61±0.10	1.50±0.20	1.52±0.27
C27:2	1.00±0.33	0.89±0.08	1.02±0.25	1.24±0.37	1.09±0.24	1.03±0.28	1.12±0.33	0.83±0.10	1.08±0.25	0.97±0.28	1.00±0.28
ΣSFA	12.81±6.94	13.27±6.95	12.05±3.19	6.68±0.41	13.16±3.93	11.91±5.69	10.46±5.03	9.79±3.87	6.98±0.78	10.78±5.32	11.33±5.53
ΣMUFA	6.82±3.19	6.50±4.23	5.56±1.84	2.93±0.41	5.98±1.73	5.77±3.08	4.59±2.08	4.41±2.14	6.11±2.25	5.72±2.97	5.74±3.03
ΣPUFA	4.02±6.23	10.24±4.99	11.47±3.89	7.99±1.37	13.42±2.92	11.57±4.94	9.80±4.52	9.29±2.65	12.97±3.61	11.91±5.65	11.74±5.32
ΣHUFA	7.26±1.43	7.36±3.18	5.91±1.13	4.56±0.72	9.08±2.44	6.83±2.43	5.79±1.54	6.78±2.05	6.89±1.88	6.65±1.74	6.74±2.11
Σn-3	5.02±1.02	5.07±2.32	4.36±0.71	3.34±0.57	6.26±1.28	4.81±1.62	4.05±1.00	4.78±1.48	5.10±1.23	4.77±1.23	4.79±1.43
Σn-6	19.26±7.49	15.54±7.48	15.35±4.74	10.35±0.73	20.00±5.33	16.28±6.76	13.55±5.98	13.97±4.23	17.41±5.34	16.49±7.00	16.38±6.88
Σn-7	1.99±1.29	1.98±1.70	1.69±0.67	0.41±0.08	1.70±0.84	1.65±1.25	1.13±0.97	1.06±0.83	1.76±0.85	1.67±1.27	1.66±1.26
Σn-9	10.76±4.95	7.90±4.85	8.67±2.99	5.33±1.02	9.89±2.55	8.68±4.20	7.45±3.41	7.42±3.11	10.10±3.69	9.25±4.66	8.97±4.45
EPA/DHA	0.06±0.02	0.15±0.15	0.07±0.02	0.09±0.03	0.05±0.01	0.09±0.08	0.08±0.05	0.07±0.03	0.07±0.01	0.07±0.03	0.08±0.06
ARA/EPA	6.79±1.18	6.27±3.73	6.53±2.19	5.50±0.60	7.84±0.83	6.57±2.32	6.81±2.17	8.02±3.70	5.71±1.76	6.87±2.27	6.72±2.30
Σn-6/Σn-3	3.72±0.78	3.06±0.67	3.44±0.51	3.21±0.68	3.15±0.21	3.34±0.67	3.24±0.60	2.93±0.10	3.36±0.37	3.35±0.70	3.35±0.69
ΣTotal FA	40.91±16.79	37.37±18.72	34.98±9.80	22.17±1.67	41.63±11.01	36.08±15.15	30.64±13.03	30.28±10.50	32.96±6.81	35.05±14.14	35.56±14.65

Table S2. Fatty acid profile ($\mu\text{g}\cdot\text{mg}^{-1}$ dry tissue weight, mean \pm SD) of *A. ocellaris* liver tissue at different temperature conditions (26 °C vs 30 °C) and timepoints (T0, T7, T14, T21, T28), N_{total} = 38 specimens.

LIVER	Overall control	30 °C										Overall liver
		26 °C					30 °C					
		T0	T7	T14	T21	T28	Overall 26 °C	T7	T14	T21	T28	
C14:0	1.68±0.80	0.64±0.47	3.34±2.79	0.90±0.25	0.96±0.43	1.61±1.58	0.75±0.42	4.99±1.88	1.07±0.20	0.42±0.12	1.94±1.90	1.78±1.69
C15:0	0.51±0.19	0.51±0.17	0.51±0.10	0.53±0.02	0.51±0.16	0.51±0.15	0.44±0.10	0.75±0.28	0.48±0.17	0.35±0.07	0.52±0.23	0.52±0.19
C16:1n7	5.56±2.69	2.25±1.74	13.79±13.14	2.93±1.45	3.07±1.05	6.00±5.02	1.96±1.02	14.00±8.91	5.34±0.76	1.43±0.33	6.06±5.42	6.03±5.25
C16:0	32.31±15.32	26.25±7.20	38.94±13.81	20.03±12.37	32.77±7.01	30.76±13.45	26.26±14.10	62.23±33.18	39.76±4.41	25.83±1.42	38.21±23.36	34.57±19.53
C17:1n7	1.14±0.46	0.89±0.47	1.60±0.56	0.78±0.33	1.04±0.45	1.12±0.55	0.62±0.41	2.21±0.74	0.98±0.30	0.58±0.17	1.16±0.77	1.14±0.68
C17:0	0.95±0.33	1.15±0.38	1.20±0.34	1.49±0.08	1.49±0.04	1.21±0.36	1.31±0.30	1.41±0.40	1.30±0.47	1.46±0.20	1.27±0.40	1.24±0.38
C18:2n6c	4.66±2.10	3.78±2.56	5.13±1.06	5.61±2.32	5.37±1.27	4.80±2.07	5.33±3.25	7.97±3.48	8.36±2.65	3.01±0.42	6.01±3.33	5.42±2.85
C18:2n6t + C18:1n9c ³	12.79±4.60	7.45±5.72	15.39±8.38	4.34±3.54	13.29±4.47	11.00±7.04	10.61±5.63	26.49±10.38	17.98±4.83	7.86±0.95	15.68±9.19	13.39±8.54
C18:1n9t	5.29±2.30	5.23±2.02	7.73±2.15	5.45±0.56	7.00±1.83	6.12±2.23	5.69±2.22	9.49±3.96	6.48±1.55	4.30±0.44	6.42±3.09	6.27±2.71
C18:0	12.02±3.68	13.74±2.54	15.07±2.14	10.08±6.10	15.66±1.01	13.40±3.84	14.44±0.92	14.67±1.97	13.58±2.34	13.41±1.15	13.65±2.51	13.52±3.23
C19:1n9	0.18±0.05	0.36±0.18	0.35±0.19	0.35±0.05	0.22±0.04	0.29±0.15	0.29±0.09	0.27±0.08	0.30±0.09	0.35±0.01	0.27±0.09	0.28±0.13
C20:5n3	1.10±0.60	0.94±0.85	1.63±1.00	1.14±0.37	1.71±0.04	1.28±0.78	1.72±0.48	2.18±0.74	0.87±0.27	0.93±0.33	1.42±0.74	1.35±0.76
C20:4n6 (ARA)	1.29±0.55	1.14±0.76	1.55±0.49	1.37±0.37	1.67±0.17	1.38±0.57	2.11±0.35	1.89±0.34	1.38±0.63	1.21±0.38	1.62±0.59	1.50±0.59
C20:3n3 + C20:3n6 ⁴	0.84±0.43	0.63±0.33	2.00±1.14	0.63±0.24	0.85±0.06	1.04±0.83	0.80±0.08	4.04±1.24	1.35±0.25	0.71±0.21	1.64±1.47	1.34±1.23
C20:1n9	3.58±2.01	3.14±1.57	4.72±1.00	3.76±0.69	5.24±1.53	4.01±1.66	3.41±2.24	4.38±1.83	4.24±2.19	2.32±0.26	3.67±2.03	3.84±1.87
C20:0	0.34±0.07	0.44±0.06	0.43±0.12	0.38±0.06	0.36±0.00	0.39±0.09	0.45±0.06	0.46±0.14	0.32±0.11	0.39±0.02	0.40±0.11	0.39±0.10
C22:6n3 (DHA)	1.94±0.87	1.98±1.92	2.47±2.35	2.39±0.49	2.75±0.16	2.26±1.58	3.33±0.83	3.03±0.67	2.52±0.90	2.61±0.33	2.70±0.92	2.48±1.30
C22:5n3 (EPA)	0.52±0.24	0.63±0.27	0.74±0.27	0.92±0.33	0.95±0.02	0.72±0.30	1.90±1.13	0.86±0.59	1.19±0.31	1.28±0.38	1.15±0.80	0.94±0.65
C22:4n6	0.77±0.52	0.67±0.47	0.93±0.43	0.92±0.42	1.21±0.04	0.87±0.46	1.80±1.55	1.56±0.25	0.99±0.44	1.11±0.25	1.27±0.91	1.07±0.75

^{3,4} These FA have the same retention time and are eluted in a single merged peak in the GC.

C22:2n6	2.37±1.58	1.31±0.94	2.82±0.51	2.01±0.44	2.27±1.44	2.16±1.22	1.80±0.91	3.22±1.25	2.87±0.57	1.13±0.22	2.36±1.29	2.26±1.26
C22:0	0.27±0.07	0.42±0.09	0.35±0.11	0.35±0.10	0.34±0.06	0.35±0.10	0.56±0.21	0.53±0.34	0.45±0.20	0.52±0.04	0.46±0.24	0.40±0.19
C24:1n9	1.57±0.74	1.68±0.21	2.04±0.73	1.79±0.16	1.98±0.35	1.80±0.57	1.77±0.21	1.90±0.65	1.90±0.54	1.80±0.06	1.78±0.55	1.79±0.56
C26:2n6	5.72±1.33	6.36±2.72	6.69±1.74	7.95±0.87	7.03±0.27	6.61±1.87	5.77±2.38	7.90±2.76	6.87±1.61	9.54±0.31	6.96±2.38	6.79±2.16
C27:2	3.58±1.00	4.68±0.26	4.43±1.33	3.80±0.92	4.22±0.05	4.17±0.99	4.12±0.83	5.05±1.59	2.80±1.40	4.19±0.17	3.98±1.37	4.07±1.20
ΣSFA	48.07±18.85	43.15±9.96	59.85±11.60	33.74±12.72	52.10±8.72	48.23±15.64	44.20±15.04	85.06±31.44	56.95±6.69	42.37±2.28	56.44±25.08	52.43±21.40
ΣMUFA	17.31±5.65	13.55±5.84	30.22±15.23	15.06±2.53	18.55±5.23	19.35±10.75	13.74±5.87	32.25±11.92	19.26±3.86	10.78±1.11	19.36±10.30	19.35±10.53
ΣPUFA	29.96±9.77	24.22±9.63	36.46±7.51	24.34±2.84	33.03±7.46	29.78±9.54	28.43±9.30	54.66±17.94	40.23±10.23	26.45±2.01	36.62±15.81	33.28±13.56
ΣHUFA	5.61±2.71	5.37±4.16	7.32±4.34	6.74±1.87	8.28±0.10	6.50±3.46	10.86±1.65	9.53±1.97	6.94±2.46	7.13±1.58	8.16±2.92	7.35±3.30
Σn-3	4.39±2.07	4.19±3.25	6.83±3.76	5.09±1.36	6.25±0.06	5.29±2.89	7.76±0.97	10.11±1.44	5.92±1.42	5.53±1.19	6.91±2.55	6.12±2.84
Σn-6	30.38±9.97	23.33±12.81	36.98±8.98	25.22±4.58	34.44±7.56	30.12±11.02	31.55±9.38	56.10±16.65	42.32±11.29	27.18±2.38	38.22±15.68	34.26±14.20
Σn-7	6.69±2.85	3.14±2.19	15.38±13.69	3.71±1.75	4.11±1.50	7.12±6.46	2.58±1.42	16.21±9.25	6.33±0.70	2.02±0.47	7.22±7.00	7.17±7.75
Σn-9	23.41±9.27	17.86±8.71	30.23±9.86	15.69±2.95	27.73±8.21	23.22±10.10	21.77±10.03	42.53±13.77	30.92±8.50	16.62±1.55	27.82±13.41	25.58±12.13
EPA/DHA	0.27±0.04	0.52±0.27	1.13±1.37	0.37±0.08	0.35±0.02	0.56±0.76	0.73±0.73	0.26±0.16	0.49±0.06	0.48±0.11	0.45±0.40	0.50±0.60
ARA/EPA	2.60±0.62	1.83±0.71	2.27±0.66	1.57±0.23	1.76±0.19	2.07±0.68	1.37±0.51	3.36±1.79	1.14±0.32	0.95±0.13	1.93±1.31	2.00±1.06
Σn-6/Σn-3	7.84±3.67	6.39±1.81	7.15±4.01	5.26±1.49	5.52±1.27	6.63±3.04	4.14±1.34	5.49±1.03	7.14±0.79	5.16±1.18	5.94±2.44	6.28±2.77
ΣTotal	100.95±33.97	86.29±25.54	133.85±18.50	79.88±14.44	111.96±21.52	103.86±31.44	97.24±28.41	181.50±30.70	123.38±22.19	86.73±5.12	120.57±44.32	112.41±39.47

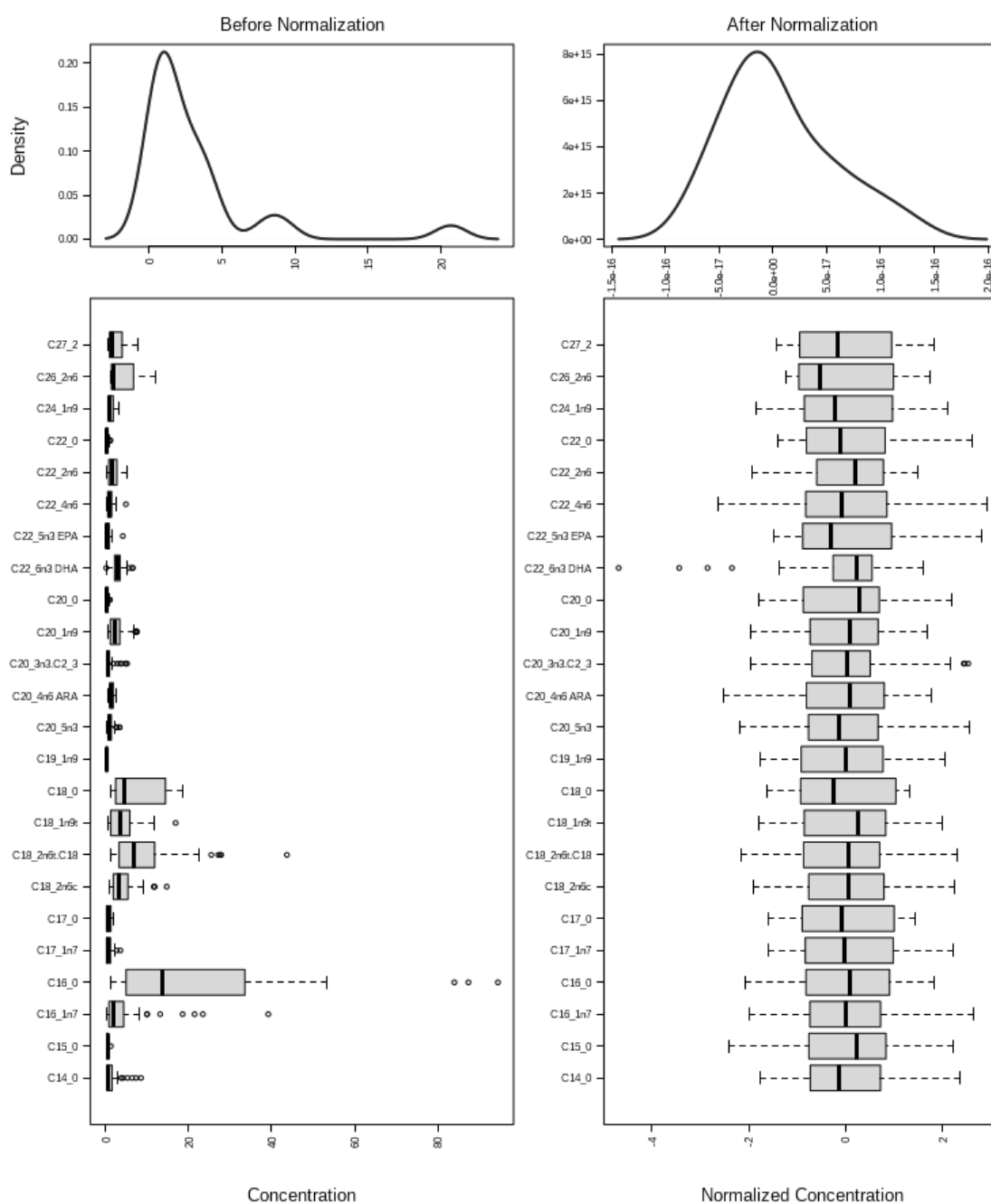


Figure S1. Fatty acid concentration ($\mu\text{g}.\text{mg}^{-1}$ dry weight, distribution, and variance) before and after normalization procedure (log transformed and auto-scaled – mean centered and divided by the standard deviation of each variable).

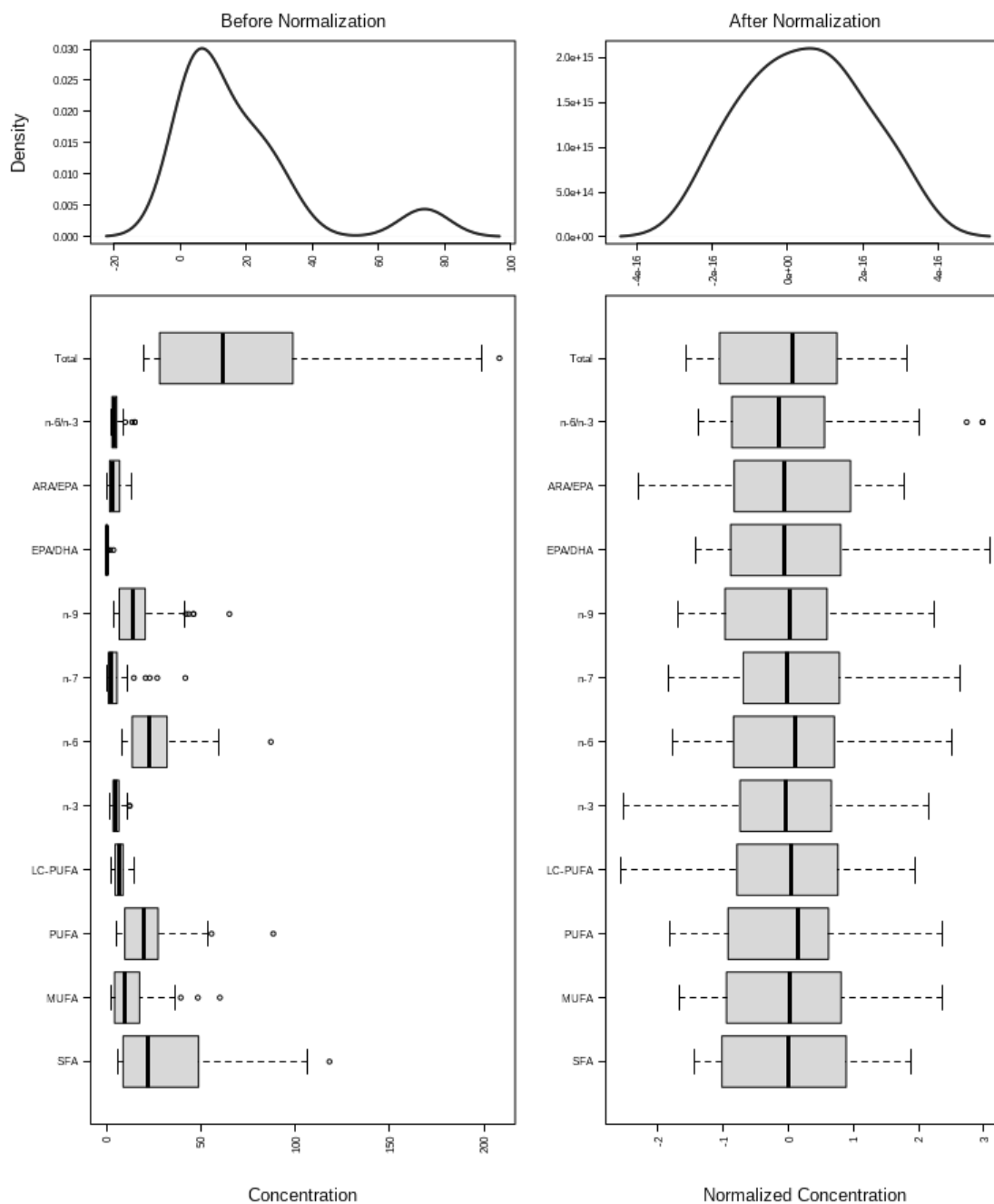


Figure S2. Fatty acid classes concentration ($\mu\text{g}.\text{mg}^{-1}$ dry weight) and fatty acid ratios (distribution and variance) before and after normalization procedure (log transformed and auto-scaled – mean centered and divided by the standard deviation of each variable).

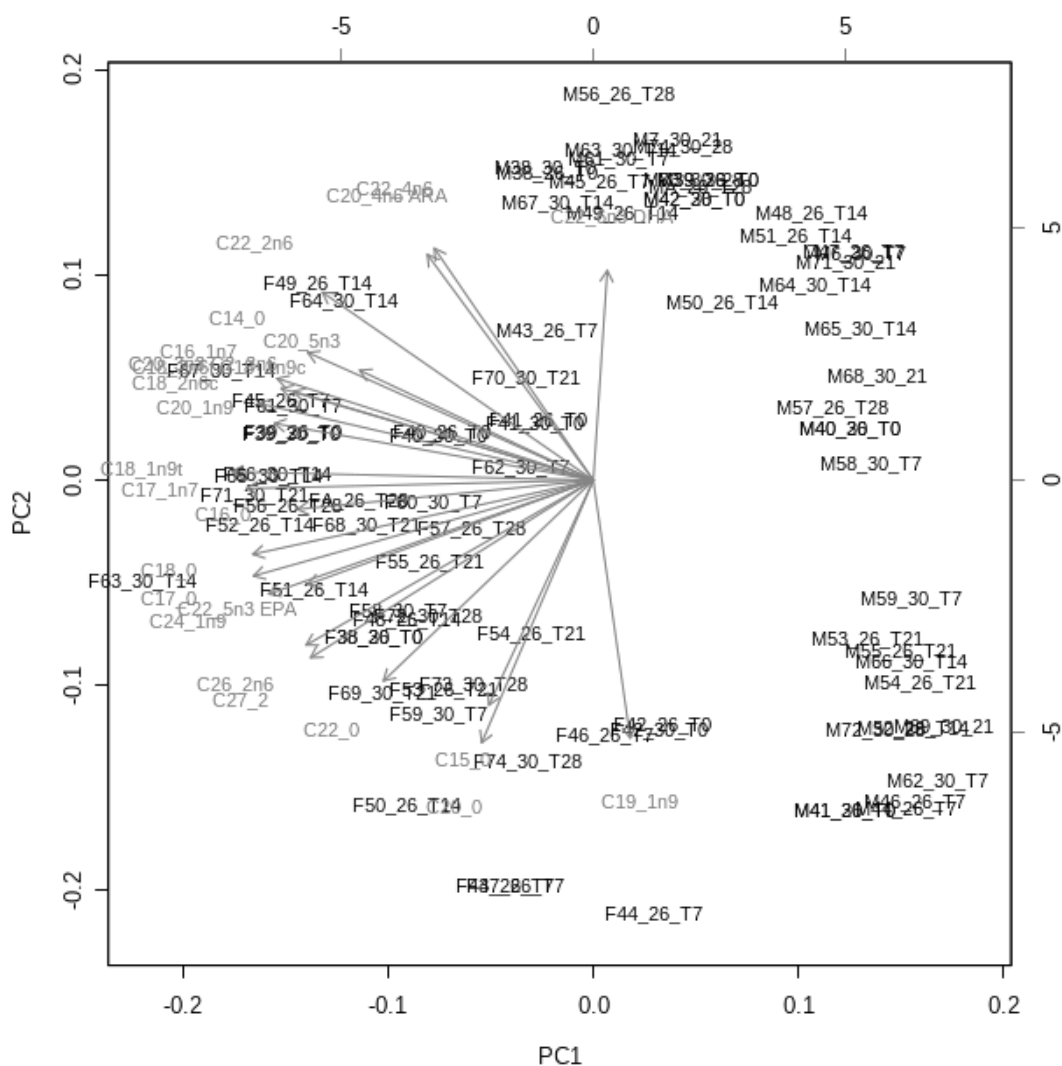


Figure S3. PCA biplot of samples scores (black) and fatty acids' loadings (vectors in red). The further away the vectors are from a PC origin, the more influence they have on that PC. Small angles between vectors imply positive correlation between them, whereas large angles suggest negative correlation and a 90° angle indicates no correlation between two fatty acids.

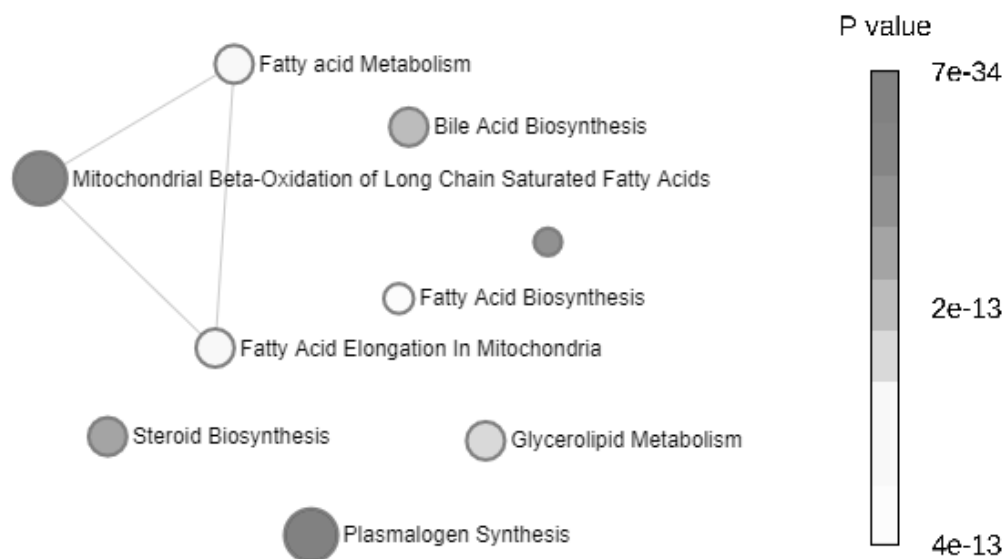


Figure S4. Functional network for enriched FA set for differences between muscle vs liver. Each node represents a metabolite set with its colour based on its p-value (FDR corrected) and its size is based on the number of hits (FA). Two metabolite sets are connected by an edge if the number of their shared metabolites is over 25 % of the total number of their combined metabolite sets.

Table S3. Results from quantitative enrichment analysis. The Q-statistic for a metabolite set is the average of the Q-statistics for each metabolite in the set. This table is complementary to Fig. 4A in the main text. Relative abundance of the relevant listed FA was significantly higher in liver when compared to muscle, except for C18:2n-6c (linoleic acid).

Metabolic pathway	Total compounds	Hits	FA	Q-stat	Raw p-value	FDR	SMPD Library Reference
<i>Plasmalogen synthesis</i>	26	1	C18:0	83.67	8.30E-35	3.73E-34	https://smpdb.ca/view/SMP0000479
<i>Mitochondrial β-oxidation of LC-SFA</i>	28	1	C18:0	83.67	8.30E-35	3.73E-34	http://www.smpdb.ca/view/SMP000482
<i>α-Linolenic acid and linoleic acid metabolism</i>	19	5	C18:2n-6c C20:5n-3 C20:3n-6 C22:6n-3 C22:5n-3	31.76	3.84E-16	1.15E-15	http://www.smpdb.ca/view/SMP000018
<i>Steroid biosynthesis</i>	48	1	C16:0	53.35	1.45E-15	1.63E-15	http://www.smpdb.ca/view/SMP000023
<i>Bile acid biosynthesis</i>	65	1	C16:0	53.35	1.45E-15	1.63E-15	http://www.smpdb.ca/view/SMP000035
<i>Glycerolipid metabolism</i>	25	1	C16:0	53.35	1.45E-15	1.63E-15	http://www.smpdb.ca/view/SMP000039
<i>Fatty acid metabolism</i>	43	1	C16:0	53.35	1.45E-15	1.63E-15	http://www.smpdb.ca/view/SMP000051
<i>Fatty acid elongation in mitochondria</i>	35	1	C16:0	53.35	1.45E-15	1.63E-15	http://www.smpdb.ca/view/SMP000054
<i>Fatty acid biosynthesis</i>	35	2	C14:0 C16:0	36.21	3.60E-13	3.60E-13	https://smpdb.ca/view/SMP0000456

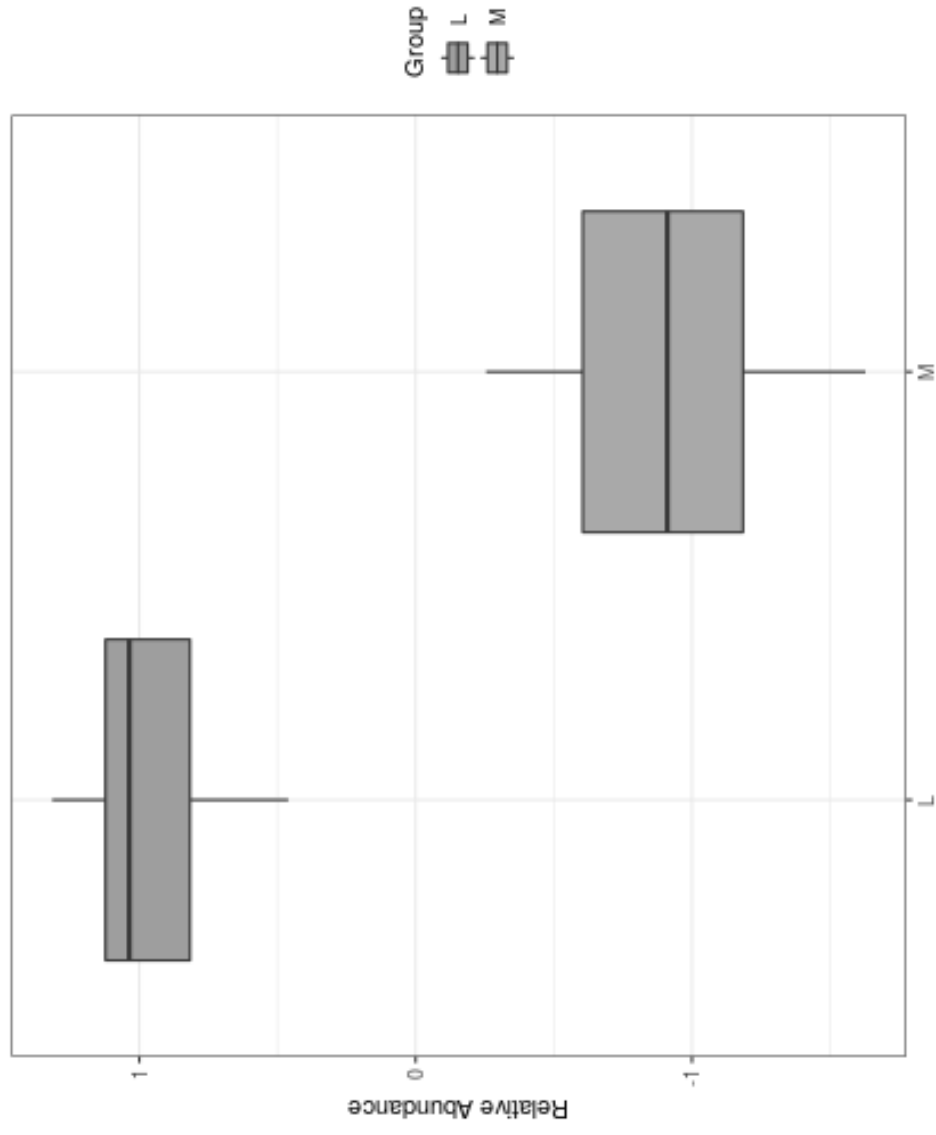


Figure S5. Relative abundance of C18:0 (stearic acid) in liver and muscle. C18:0 is involved in two key biological pathways: (i) plasmalogen synthesis and (ii) mitochondrial β -oxidation of long chain saturated fatty acids.

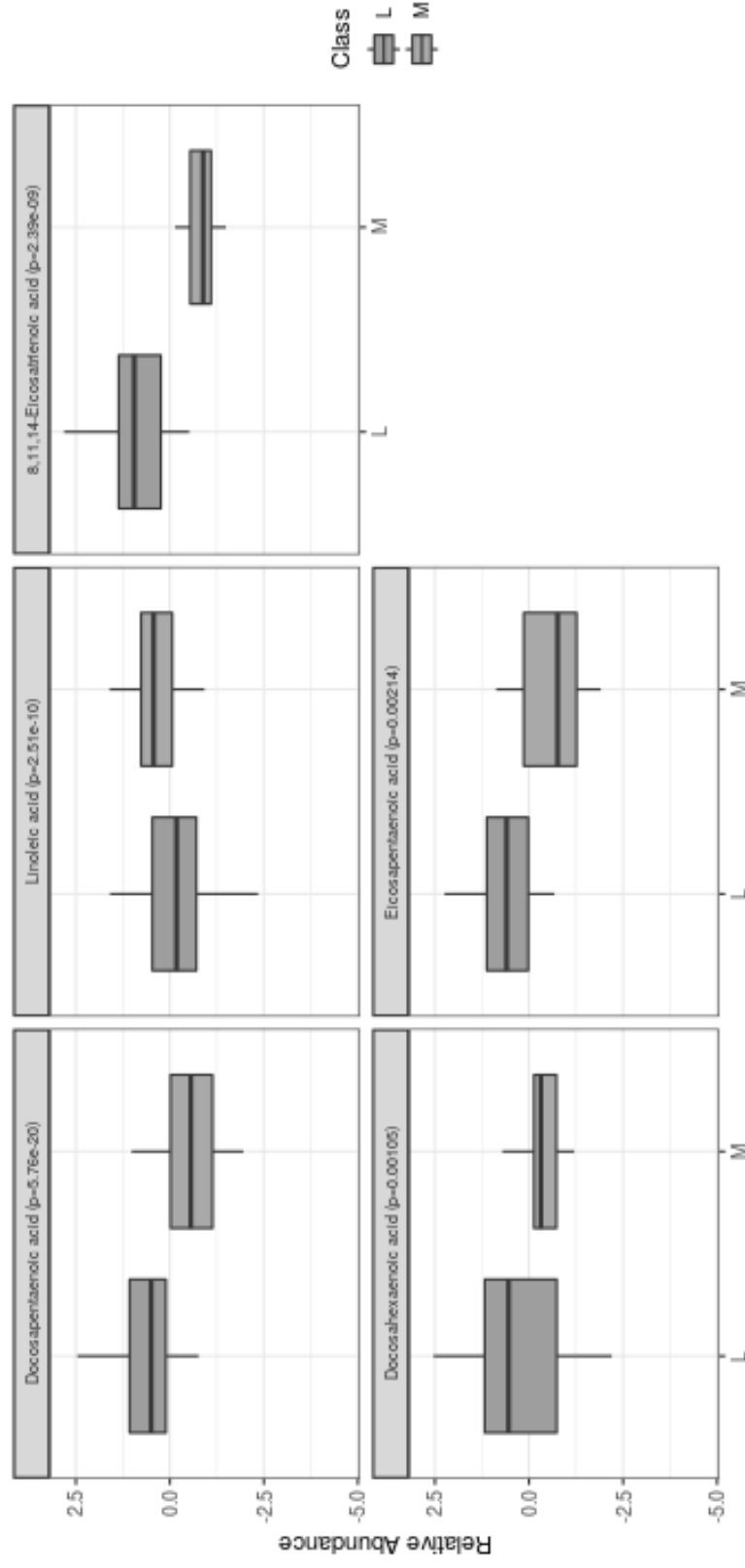


Figure S6. Relative abundance of C22:5n-3 (Docosapentaenoic acid), C18:2n-6c (linoleic acid), C20:3n-6 (8Z,12E,14Z-eicosatrienoic acid), C22:6n-3 (Docosahexaenoic acid) and C20:5n-3 (eicosapentaenoic acid) in liver and muscle. These FA are involved in one key biological pathway: (i) α -Linolenic acid and linoleic acid metabolism. P-values of Q-statistic for each individual metabolite.

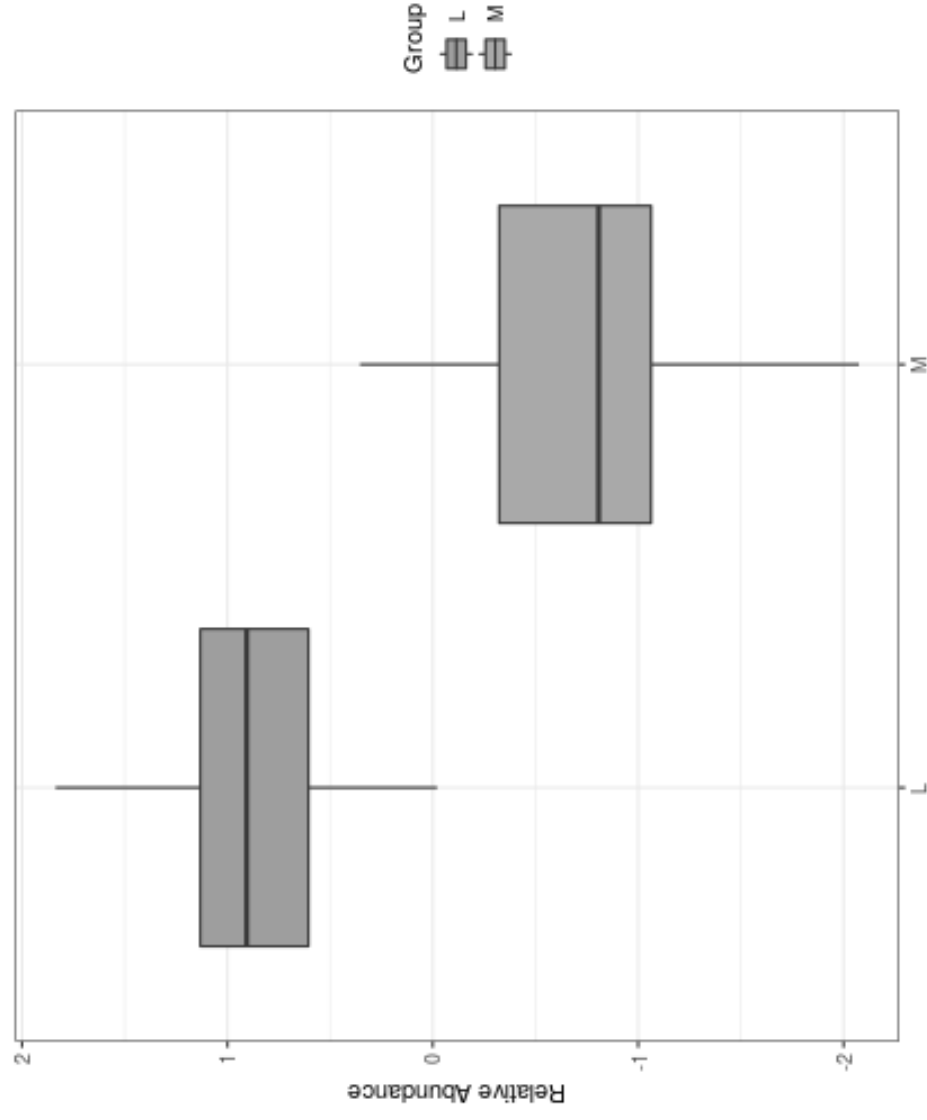


Figure S7. Relative abundance of C16:0 (palmitic acid) in liver and muscle. C16:0 is involved in several key biological pathways: (i) steroid biosynthesis, (ii) bile acid biosynthesis, (iii) glycerolipid metabolism, (iv) fatty acid metabolism, (v) fatty acid elongation in mitochondria

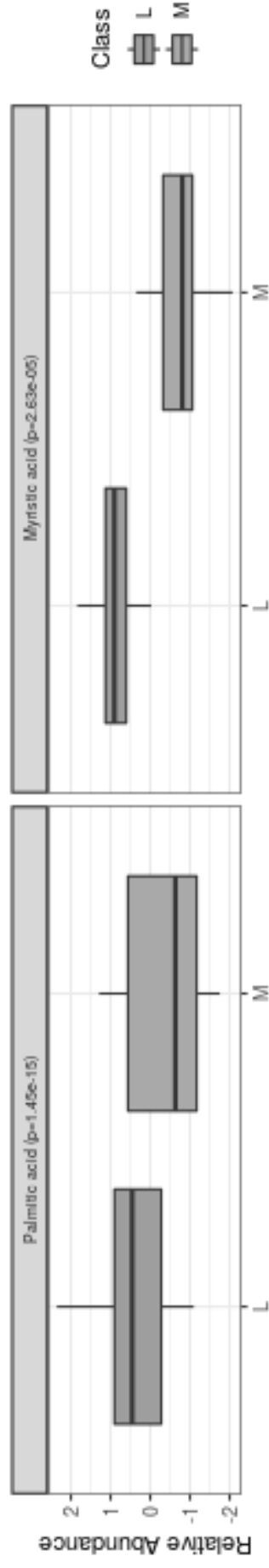


Figure S7. Relative abundance of C16:0 (palmitic acid) and C14:0 (myristic acid) in liver and muscle. These two FA are involved in a key biological pathway: (i) fatty acid biosynthesis. P-values of Q-statistic for each individual metabolite.